



Designing of a multi-epitope vaccine candidate against Nipah virus by *in silico* approach: a putative prophylactic solution for the deadly virus

Prativa Majee, Neha Jain & Amit Kumar

To cite this article: Prativa Majee, Neha Jain & Amit Kumar (2021) Designing of a multi-epitope vaccine candidate against Nipah virus by *in silico* approach: a putative prophylactic solution for the deadly virus, Journal of Biomolecular Structure and Dynamics, 39:4, 1461-1480, DOI: [10.1080/07391102.2020.1734088](https://doi.org/10.1080/07391102.2020.1734088)

To link to this article: <https://doi.org/10.1080/07391102.2020.1734088>



[View supplementary material](#)



Published online: 04 Mar 2020.



[Submit your article to this journal](#)



Article views: 924



[View related articles](#)



[View Crossmark data](#)



Citing articles: 8 [View citing articles](#)



Designing of a multi-epitope vaccine candidate against Nipah virus by *in silico* approach: a putative prophylactic solution for the deadly virus

Prativa Majee , Neha Jain  and Amit Kumar 

Discipline of Biosciences and Biomedical Engineering, Indian Institute of Technology Indore, Indore, Simrol, Indore, India

Communicated by Ramaswamy H. Sarma

ABSTRACT

Nipah virus (NPV) is one of the most notorious viruses with a very high fatality rate. Because of the recurrent advent of this virus and its severe neurological implications, often leading to high mortality, the WHO R&D Blueprint, 2018 has listed the Nipah virus as one of the emerging infectious diseases requiring urgent research and development effort. Yet there is a major layback in the development of effective vaccines or drugs against NPV. In this study, we have designed a stable multivalent vaccine combining several T-cell and B-cell epitopes of the essential Nipah viral proteins with the help of different ligands and adjuvants which can effectively induce both humoral and cellular immune responses in human. Different advanced immune-informatic tools confirm the stability, high immunogenicity and least allergenicity of the vaccine candidate. The standard molecular dynamic cascade analysis validates the stable interaction of the vaccine construct with the human Toll-like receptor 3 (TLR3) complex. Later, codon optimization and *in silico* cloning in a known pET28a vector system shows the possibility for the expression of this vaccine in a simple organism like *E.coli*. It is believed that with further *in vitro* and *in vivo* validation, this vaccine construct can pose to be a better prophylactic solution to the Nipah viral disease.

Abbreviation: CTL: Cytotoxic T-cell; HTL: Helper T Lymphocytes; MHC: Major Histocompatibility Complex; MD: Molecular Dynamics; NPV: Nipah virus; TLR: Toll-Like Receptor

ARTICLE HISTORY

Received 30 July 2019
Accepted 17 February 2020

KEYWORDS

Vaccine; multi-epitopes;
Nipah virus; Toll-like
Receptor 3; immuno-
informatics

1. Introduction

Nipah virus, one of the newly emerging deadly viruses belongs to the Paramyxoviridae family sharing the Henipavirus genus with another prototype virus of the genus, named Hendra virus (Chua et al., 2000). The first outbreak of the Nipah virus dates back to 1998 in Malaysia and then subsequently in Singapore, Bangladesh, India, and the Philippines, especially targeting the South-east Asian countries. Since 2001, Bangladesh has witnessed almost annual outbreaks of Nipah virus. In the recent breakout in Kerala, India (May, 2018) about 23 cases were reported out of which only two patients survived, resulting in 91% case-fatality rate (People et al., 2018). The fruit bat (*Pteropus* species) acts as the natural reservoir for this virus, while spillover to other animals like pigs and humans results in the transmission of this zoonotic virus to wider host ranges; partly because it uses the highly conserved mammalian receptors, ephrin B2/B3 for the viral entry (Clayton, 2017; Weatherman, Feldmann, & de Wit, 2018). The broad host range, high virulence and the consequential morbidity and mortality due to the Nipah virus lead to its categorization as Biosafety Level 4 virus. Moreover, its high potential to act as a bioterrorism agent demarcates it as category C pathogen (Ang, Lim, & Wang, 2018). Though the Nipah virus outbreaks are sporadic, yet

around two billion people are at risk in all countries including the ones which have already encountered the outbreaks and also those which naturally harbors the *Pteropus* bats. The typical symptoms of Nipah viral infection include fever, vomiting, headache, dizziness and may eventually lead to more serious conditions like severe encephalitis, systemic vasculitis and acute respiratory problems (Ong & Wong, 2015). The relapse or the recurrent encephalitis along with the ramification of the neurological problems aggravate the survivors' living conditions. The Nipah virus not only takes a heavy toll on the human population but largely affects the animal husbandry sector also (Ahmad, 2000; Glennon et al., 2018; Mohd Nor, Gan, & Ong, 2000).

The Nipah virus bears a negative-stranded RNA genome consisting of six essential genes, N, P, M, F, G, and L. While the G gene codes for the glycoprotein guiding the virus in host receptor recognition and attachment, the F gene codes for the fusion protein helping in fusion of the viral membrane with the host membrane. Both the glycoprotein and the fusion protein aid in viral entry to the host cells. The N gene codes for nucleoprotein which remains bound to the RNA and assists in viral genome replication and packaging. The RNA dependent RNA polymerase (RdRp) enzyme required for the RNA genome replication is translated from

the L gene. The matrix protein needed during the virus budding and assembly is encoded by the M gene. The P gene exceptionally codes not only for the phosphoprotein but also codes for three additional proteins namely, C, V, and W each having some immune modulatory role to play (Satterfield, Geisbert, & Mire, 2016; Satterfield et al., 2015). On recognition of the viral RNA by the host cytoplasmic RNA helicase like RIG-I, MDA-5, etc., the IFN responses are activated along with the chemokines (e.g. IP10) and cytokines (e.g. IL-6). The Nipah viral proteins namely, V and C proteins antagonize the innate immune response of the host cells. Notably, the N-terminal domains of the P, V and W proteins bind to the STAT1, thus inhibiting its phosphorylation and thereby hindering the JAK/STAT signaling pathway (Shaw, García-Sastre, Palese, & Basler, 2004).

With no licensed drug or vaccine available against Nipah virus infection, this virus makes a place in the list of WHO R&D Blueprint, 2018 for emerging infectious diseases requiring urgent research and development efforts (Mehand, Al-Shorbaji, Millett, & Murgue, 2018). The success of safe and effective vaccines against its close paramyxovirus members, i.e. Mumps and Measles and its average incubation period of 10 days, provide evidence that the vaccine development for the Nipah virus is feasible (Satterfield, Dawes, & Milligan, 2016). Different animal models like cats, ferrets, hamsters, African Green Monkeys, and pigs have been extensively used for testing the various vaccine candidates designed usually using the fusion and glycoprotein of Nipah virus (Bossart et al., 2012; Kong et al., 2012; Lo et al., 2014; McEachern et al., 2008; Mire et al., 2013; Prescott et al., 2015; Weingart et al., 2006). Different vaccine platforms have also been explored including the subunit vaccines, vectored vaccines using vesicular stomatitis virus (VSV), rabies virus (RABV), adeno-associated virus (AAV), Newcastle disease virus (NDV), etc. as viral vectors for the vaccine development (Satterfield, Dawes, et al., 2016). Some groups have also put forward *in silico* approaches to design epitope-based vaccine candidates against the Glycoprotein, Fusion protein or the RdRp of Nipah virus (Kamthania & Sharma, 2015; Parvege, Rahman, Nibir, & Hossain, 2016; Ravichandran, Venkatesan, & Febin Prabhu Dass, 2019; C. K. Saha, Mahbub Hasan, Saddam Hossain, Asraful Jahan, & Azad, 2017; Sakib, Islam, Hasan, & Nabi, 2014). Our study stands aside from the already reported epitope-based vaccine candidates as we have effectively designed the multivalent epitope-based vaccine considering the complete antigenic proteome of the Nipah virus. Moreover, considering the crucial role of innate immune response and intestinal absorption and adsorption of the vaccine, along with the antigenic epitopes, β -defensin, and an M-cell ligand are added to the N and C-terminal end of the vaccine respectively. β -defensin activates the innate immune system leading to the generation of anti-microbial resistance on the epithelial cell surface (Oppenheim, Biragyn, Kwak, & Yang, 2003), while M-cell ligand targets the goblet cells present in the intestinal lining and helps the vaccine to cross the gut barrier (Fievez et al., 2010). Also, earlier reports depict that the Toll-like Receptor 3 (TLR3) is involved during the Nipah viral infection as it specifically identifies the dsRNA

of the virus (Shaw, Cardenas, Zamarin, Palese, & Basler, 2005). On an event of viral infection, TLR3 associates the TIR domain with a TIR domain-containing adaptor protein named TRIF, thereby signaling downstream transcription factors, nuclear factor $\kappa\beta$ (NF- $\kappa\beta$) and IFN regulator factor 3 (IRF3) essential for the IFN- β promoter activation. But, the Nipah virus inhibits this TLR3 signaling pathway by blocking the expression of IRF3. Therefore, a construct having the propensity of activating the TLR3 complex will lead to a generation of more effective and efficient vaccine construct. Henceforth, in the current approach, we have checked the propensity of the multi-epitope vaccine construct of the Nipah virus and human TLR3 complex. This epitope-based vaccine development approach has been explored and proved to be promising in a number of diseases caused by viruses like Herpes simplex virus (Hasan et al., 2019; Kumar et al., 2019), Yellow Fever Virus (Tosta et al., 2019), SARS Coronavirus (Srivastava et al., 2019), Chikungunya (Bappy et al., 2020), Dengue (Sabetian, Nezafat, Dorosti, Zarei, & Ghasemi, 2019), Alkhurma hemorrhagic fever virus (Ul-Rahman & Shabbir, 2019), etc. as well as by other pathogens including *Leishmania donovani* (Khatoon et al., 2019), *Elizabethkingia anophelis* (Nain et al., 2019), *Flavobacterium columnare* (Bhattacharya et al., 2020), *Bacillus anthracis* (Gupta, Khatoon, Mishra, Verma, & Prajapati, 2019), *Streptococcus pneumoniae* (Dorosti et al., 2019), *Helicobacter pylori* (Pasala et al., 2019), etc. Thus, this multi-epitope vaccine construct designed with a multi-dimensional approach helps in the activation of TLR3 along with the innate and specific adaptive immune response that will also be adsorbed from the intestinal lining and will generate a prominent immune response against the deadly Nipah virus.

2. Methodology

2.1. Antigenic proteome retrieval from the Nipah virus genome

The complete protein sequences of all the Nipah viral genes were retrieved from the National Center of Biotechnology Information (NCBI). The retrieved proteins were scrutinized for their antigenic property by using VaxiJen (<http://www.ddg-pharmfac.net/vaxijen/VaxiJen/VaxiJenhtml>) (Doytchinova & Flower, 2007) and Proteogen (<http://www.violinet.org/protegen/index.php>) servers. The proteins showing the antigenic propensity were then used for the epitope prediction and multivalent epitope vaccine construction.

2.2. Selection of MHC I/II supertypes depending on the maximum population coverage

Major histocompatibility complex (MHC) plays a crucial role in the binding to the epitopes and active presentation of the pathogenic antigens to the T lymphocytes of the immune system (Germain, 1994). This antigen presentation to the T lymphocytes leads to the production of B-cell mediated antibody production, macrophage activation, and cell mediated immune activation ultimately leading to viral load clearance

(Germain, 1994). Thus, MHCs play a crucial role in adaptive immunity. The genes encoding the MHCs are highly polymorphic in nature and their expression varies as per the geographical diversification and ethnicity throughout the world. Due to the presence of vast majority of MHC class I and class II complexes, and to cover the maximum world's population, population coverage of all the MHC supertypes was calculated for both the classes of MHCs. To check the population coverage of the MHCs, Population Coverage Tool available at the IEDB server (<http://tools.iedb.org/population/>) was explored (Bui et al., 2006). The best MHCs that cover the maximum world's population were taken under consideration for further prediction of the Cytotoxic T-cell (CTL) and Helper T-lymphocytes (HTL) epitopes. The population coverage of the MHCs in the NPV risked population that includes the South-east Asian countries was also predicted by the same server.

2.3. Selection of epitopes by sequence analysis

2.3.1. Cytotoxic T- cells (CTL) epitope prediction

Major histocompatibility complex class I acts as a mediator for the activation of Cytotoxic T-cells by acting as antigen presenters to the later. Cytotoxic T-cells mediate the pathogen clearance inside the host and are the major components of the adaptive immune system in humans. To represent the pathogenic antigen, the pathogen is first engulfed and then cleaved and processed inside the proteasome in the cytoplasm. After antigen processing, these antigens are transported to the endoplasmic reticulum via Transporter associated with antigen processing (TAP). Thereafter, these transported antigens bind with the binding groove of the MHC class I molecules and transported to the surface of the antigen presenting cells where they interact with the Cytotoxic T-cells and thereby activates them. The antigenic proteins were exploited for the prediction of promiscuous MHC-I binding epitopes having a high affinity for Cytotoxic T-cell activation. For this purpose, the NetCTL 1.2 server available at <http://www.cbs.dtu.dk/services/NetCTL/> was used (Larsen et al., 2007). NetCTL 1.2 integrates three algorithms that are used for the prediction of the epitopes which include the propensity of proteasomal cleavage of the C-terminal end of the peptide, and higher affinity for TAP transporters as well as for the MHC-I supertypes. These three integrated features led to the identification of the best CTL epitopes. Predictions were done for the best MHC-I supertypes that covered the maximum population. Further, the epitopes that shared the maximum number of supertypes were selected for sub-unit vaccine construction and overlapping epitopes were merged to form one common epitope.

To further check the immunogenicity of the selected CTL epitopes, class I Immunogenicity server available at IEDB (<http://tools.iedb.org/immunogenicity/>) was utilized (Calis et al., 2013). Epitopes having only the positive scores in the immunogenicity analysis were employed for multi-epitope vaccine construction.

2.3.2. Helper T-lymphocytes (HTL) epitope prediction

Major histocompatibility complex class II processes and presents the epitopes to Helper T-Lymphocytes (HTL/Th) cells. Th cell on activation leads to the generation of adaptive immunity via the production of various cytokines. They help in activating the humoral immune system by assisting B-cell mediated antibody class-switching, affinity maturation and cell-mediated immunity via activating T-cytotoxic cells and macrophages. They are also the key players in generating memory immune cells, thus making them an integral part of vaccine production against the pathogens. For the prediction of efficacious MHC class II binders that act as Helper T-Lymphocytes epitopes, MHC II prediction tool at IEDB (<http://tools.iedb.org/mhcii/>) was exploited (Wang et al., 2008). For MHC-II epitope prediction, the tool integrates various machine learning algorithms like neural network, support vector machines, Sterniolo, and CombiLib. To get the best epitopes with the highest MHC-II binding propensity to the selected MHC-II supertypes, IC₅₀ value <50 nM and the highest percentile rank were taken into consideration. The overlapping epitopes were combined.

To further activate IFN- γ cytokine production that will aid in the generation of innate and adaptive immunity against the virus, the IFN- γ tool server available at <http://crdd.osdd.net/raghava/ifnepitope/scan.php> that predicts the propensity of the MHC-II epitopes to activate the IFN- γ production was explored (Dhanda, Vir, & Raghava, 2013). The 9-mer peptides having the highest binding affinity with MHC-II complex and are IFN- γ positive were selected for multi-epitope vaccine construction.

2.3.3 B-cell epitope prediction

For the production of antibodies against a pathogen, the B-cells need to be activated by the specific antigens/epitopes. Therefore, the selected antigenic proteome of the Nipah virus was examined for the promiscuous linear B-cell epitopes by using the BCPRED server available at <http://ailab.ist.psu.edu/bcpred/> (El-Manzalawy, Dobbs, & Honavar, 2008). The BCPRED server takes Fasta sequence as input and generates 20mer epitopes with the default specificity of 75% towards the B-cell receptors. The epitope with the highest score was selected for further multi-epitope vaccine construction.

2.4. Structure analysis of the selected MHC I/II epitopes with the respective HLA molecules

The epitopes selected from the sequence analysis of the antigenic proteins of the Nipah virus were further evaluated for their efficacy against the selected HLA molecules by using structural analysis. The selected peptides were blind docked with the MHC I/II complex structures to check the binding site of the predicted epitopes.

For this analysis, the tertiary structures of MHC-I and MHC-II complexes were downloaded from the PDB database available at <https://www.rcsb.org/>. Similarly, the structures of the available Nipah proteins were also retrieved from the PDB database while those that were not available in the database were modeled *in silico* by using the I-TASSER server (<https://zhanglab.ccmb.med.umich.edu/I-TASSER/>) (Yang et al., 2015). I-TASSER

builds the model by threading and ab-initio protein modelling approach. These modelled proteins were then further refined by the GALAXYREFINE tool (Heo, Park, & Seok, 2013).

Next, from the protein structure files, the CTL and HTL epitope coordinates were retrieved by using the PyMOL and used as ligands in protein-peptide docking. The docking analysis was performed by using the ClusPro server (Kozakov et al., 2017). The epitopes that had the highest binding affinity and interacted with the binding groove of the HLA complexes were utilized for further analysis.

2.5. Designing of the multi-epitope vaccine construct

For the generation of a multi-epitope vaccine against the Nipah virus, the selected CTLs, HTLs and linear B-cell epitopes were threaded into a single peptide. For the efficacious innate and adaptive immune response, the β -actin adjuvant was inserted at the N-terminal region of the vaccine construct, while a universal memory T-helper cell adjuvant (TpD) was added between CTL and HTL epitopes. For the efficient intake of the vaccine construct from the gut environment, another adjuvant specific for M-cells of the intestine was inserted at the C-terminal region (Fievez et al., 2010). All the three adjuvants were separated from the epitopes by using the EAAAK linkers. For the proper orientation and structure coordinates, the AAY linkers were used between each epitope of the CTL, the GGGGS linker between the HTL epitopes while the KK linker separated the B-cell epitopes from each other.

2.6. Antigenicity/immunogenicity and allergenicity determination of the multi-epitope vaccine construct

To evaluate the antigenicity and immunogenicity of the constructed vaccine product, we exploited the VaxiJen (<http://www.ddgpharmfac.net/vaxijen/VaxiJen/>) and SCRATCH (<http://scratch.proteomics.ics.uci.edu/>) servers (Doytchinova & Flower, 2007; Magnan et al., 2010). Similarly, for the analysis of allergenicity, two servers namely, the AllerTop v 2.0 available at <http://www.ddgpharmfac.net/AllerTOP/>, and the AlgPred available at <http://crdd.osdd.net/raghava/algpred/> were used (Dimitrov, Bangov, Flower, & Doytchinova, 2014; S. Saha & Raghava, 2006).

2.7. Physicochemical analyses of the predicted multi-epitope vaccine construct

For the evaluation of physicochemical properties of the vaccine construct like instability index, aliphatic and aromatic index, hydrophobicity/hydrophilicity, etc., ProtParam tool available at <https://web.expasy.org/protparam/> was utilized (Wilkins et al., 1999).

2.8. Structure prediction and refinement of the multi-epitope vaccine construct

To check the propensity of alpha-helix, beta-sheet and coils/turns formation in the constructed vaccine product, the secondary structure of the vaccine construct was predicted by

using the PSIPRED server (<http://bioinf.cs.ucl.ac.uk/index.php>). The PSIPRED server utilizes the Position Specific Iterated - BLAST algorithm for secondary structure prediction (McGuffin, Bryson, & Jones, 2000).

Further, for tertiary structure prediction, the I-TASSER server was utilized (Yang et al., 2015). The best generated model was evaluated by visualizing its Ramachandran plot constructed by using the PROCHECK (<http://servicesn.mbi.ucla.edu/PROCHECK/>) server (Laskowski, MacArthur, Moss, & Thornton, 1993). Thereafter, GALAXY REFINE server was utilized for the refinement of the predicted tertiary structure of the multi-epitope vaccine construct (Heo et al., 2013). The refined structure with maximum residues in the favorable region of the Ramachandran plot was used for further analysis.

2.9. Stability enhancement of the vaccine construct by using disulfide engineering

After refinement of the tertiary structure, the vaccine construct was evaluated for disulfide engineering by using the Disulfide tool of Design 2 server available at <http://cptweb.cpt.wayne.edu/DbD2/> (Craig & Dombkowski, 2013). On the basis of C_{α} - C_{β} - S_{γ} , chi3 angles and the minimum energy, the residues were selected for disulfide engineering. To check the stability effect of disulfide engineering on the vaccine construct, the Eris server (<https://dokhlab.med.psu.edu/eris/>) was explored (Yin, Ding, & Dokholyan, 2007).

2.10. Interaction analysis of the multi-epitope vaccine construct with TLR-3

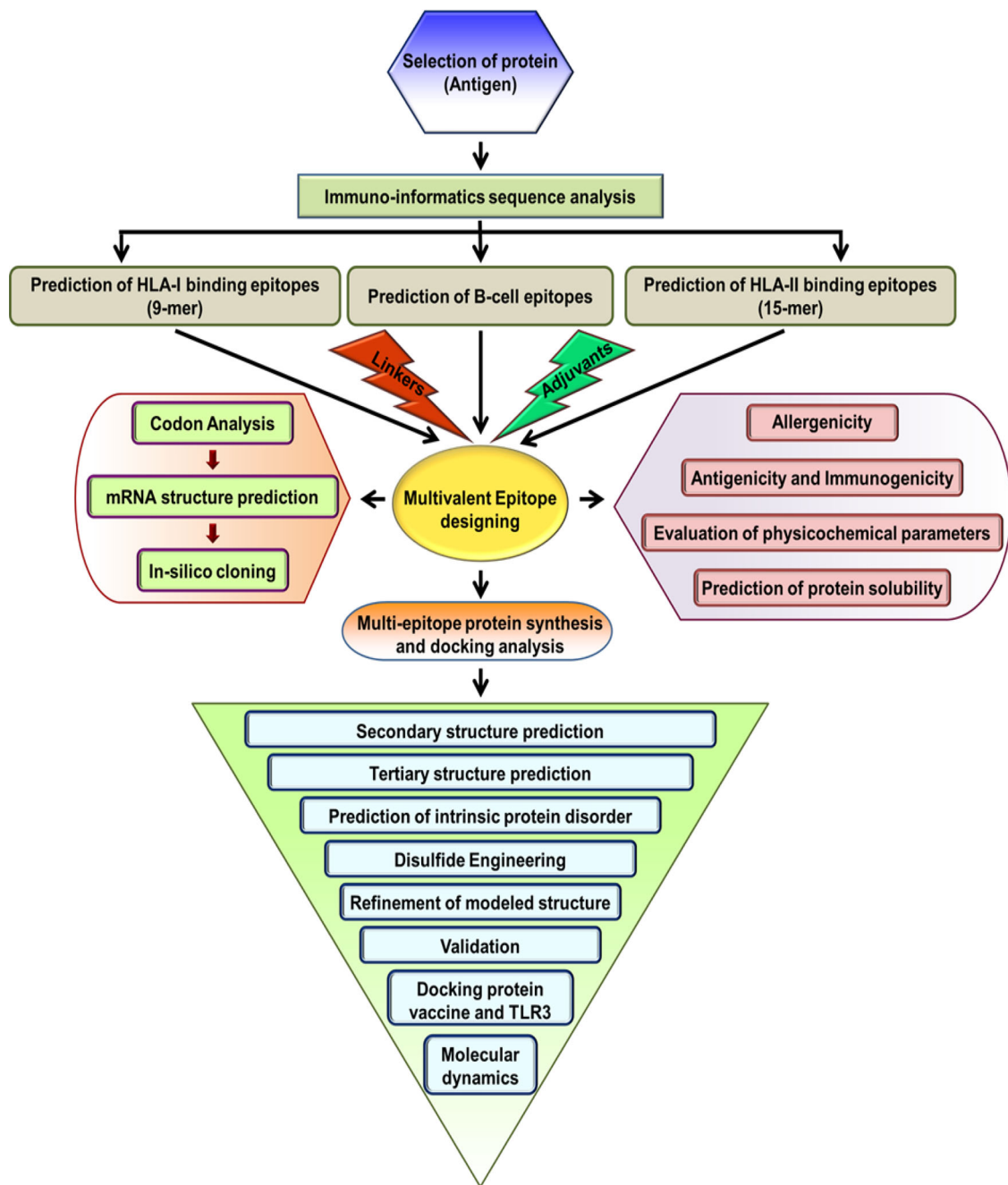
To check the interaction between the multi-epitope vaccine construct of the Nipah virus and TLR3 of human, docking analysis was performed by using the ClusPro server (Kozakov et al., 2017). The structure coordination file of TLR3 was retrieved from the PDB database and prepared for docking analysis by using the PyMol visualization tool. The docked complex structure with the minimum binding energy was used for molecular dynamics analysis.

2.11. Molecular dynamic simulation of the vaccine construct and the vaccine-TLR3 complex

To further check the stability of the multi-epitope vaccine construct and the vaccine-TLR3 complex, molecular dynamics (MD) simulation was performed using the NAMD source code (Phillips et al., 2005). For the generation of the input files (pdb and psf), psfgen script was utilized by using the VMD tool. The vaccine and vaccine-TLR3 complex was embedded in a water sphere and was used for MD analysis. At first, 10000 steps of energy minimization were performed on both the vaccine construct and vaccine-TLR3 complex. Then, the system was subsequently heated from 0 K to 310 K. Further, NPT analysis was performed followed by 50 ns molecular dynamic simulation analysis with a time step of 2 femtoseconds (fs) using Langevin dynamics algorithm. The CHARMM force field was used during the analysis, and Particle Mesh Ewald (PME) was utilized for generating the periodic boundary conditions. The trajectory

Table 1. Table showing the protein ID of the Nipah viral proteins used in our study and their corresponding VaxiJen value.

Sl. No.	Nipah Gene Name	Protein encoded by the gene	NCBI Protein ID used for analysis	VaxiJen Score
1	F	Fusion Protein	NP_112026.1	0.5017
2	G	Glycoprotein	NP_112027.1	0.5102
3	M	Matrix protein	NP_112025.1	0.4014
4	N	Nucleocapsid Protein	NP_112021.1	0.5704
5	P	Phosphoprotein	NP_112022.1	0.5874

**Figure 1.** Flowchart of the methodology used for the construction of multi-epitope vaccine for the Nipah virus.

analysis of the simulation and RMSD/RMSF analysis was performed by using TCL scripts in the VMD tool.

2.12. In silico cloning

For cDNA construction, the reverse translate tool available at the EXPASY server was used. For the optimal expression of

the vaccine construct inside the *Escherichia coli* expression system, codon analysis, and optimization, Java Codon Adaptation Tool (JCAT) was explored (Grote et al., 2005). Further, the cDNA was analyzed for the presence of restriction sites for *BamH*1 and *Hind*III and rho-independent terminator sites. Thereafter, the optimized cDNA was inserted in the PET28a (+) plasmid.

Table 2. List of final consensus epitopes of MHC-I for each viral protein with its detailed information including rescale binding affinity value, C-terminal cleavage affinity value, TAP transport efficiency score and immunogenicity score.

HLA Supertype	Position	Epitope	Predicted binding affinity	Rescale binding affinity	C-terminal cleavage affinity	TAP transport efficiency	Prediction Score	Immuno-genecity Score	Consensus Sequence
Fusion protein									
A2	272	SSYYIIVRV	0.5339	0.7959	0.9123	0.643	0.9648	0.31504	SSYYIIVRVYFPILTEIQQAYIQEL
A2	276	IIVRVVFPI	0.5224	0.7788	0.5302	0.712	0.8939	0.19452	
A2	288	IQQAYIQEL	0.5162	0.7694	0.7138	0.854	0.9192	0.08419	
A3	284	ILTEIQQAY	0.3084	0.5805	0.9667	2.786	0.8648	0.05901	
A24	273	SYYIIVRVY	0.3315	0.7058	0.9198	3.483	1.018	0.36898	
A24	274	YYIIVRVYF	0.7847	1.671	0.493	2.902	1.8901	0.29872	
A24	276	IIVRVVFPI	0.4128	0.879	0.5302	0.712	0.9942	0.19452	
A24	280	VYFPILTEI	0.6833	1.4549	0.9763	1.105	1.6566	0.23726	
B7	277	IVRVYFPIL	0.3354	0.6472	0.9012	1.174	0.841	0.23334	
B44	288	IQQAYIQEL	0.3077	0.7625	0.7138	0.854	0.9122	0.08419	
Glycoprotein									
A2	46	ILSAFNTVI	0.64	0.954	0.8389	0.674	1.1135	0.15046	ILSAFNTVIALLGSIIV
A2	55	ALLGSIVII	0.7114	1.0605	0.1852	0.725	1.1245	0.10728	
A2	56	LLGSIVIIV	0.7397	1.1027	0.279	0.329	1.161	0.20307	
A24	49	AFNTVIALL	0.3533	0.7524	0.5075	1.226	0.8898	0.22898	
B7	48	SAFNTVIAL	0.3704	0.7147	0.9344	1.22	0.9158	0.24333	
Matrix protein									
A2	335	FMIYDDVFI	0.8342	1.2435	0.0624	0.463	1.276	0.1852	QPSIPREFMIYDDVFDINTGRI
A3	330	SIPREFMIY	0.2851	0.5367	0.9334	2.946	0.824	0.18574	
A24	341	VFIDNTGRI	0.4784	1.0186	0.781	0.694	1.1704	0.045	
B7	328	QPSIPREFM	0.5127	0.989	0.248	0.057	1.0291	0.10648	
B44	333	REFMIYDDV	0.614	1.5216	0.2676	0.39	1.5812	0.15179	
Nucleocapsid protein									
A2	296	SLMLLYREI	0.4843	0.7219	0.3604	0.773	0.8146	0.01974	SLMLLYREIGPRAPYMLLEESIQ
A2	310	YMLVLEESI	0.588	0.8765	0.6842	0.569	1.0076	0.07353	TKFAPGGYPLLWSFAMGVATTI
A2	312	VLEESIQT	0.491	0.7319	0.8074	-0.57	0.8245	0.08356	
A2	322	FAPGGYPLL	0.4306	0.6419	0.8815	0.998	0.824	0.04418	
A2	333	FAMGVATTI	0.5134	0.7652	0.9414	0.611	0.937	0.10957	
A3	299	LLYREIGPR	0.5105	0.9609	0.2688	1.731	1.0877	0.29578	
A3	313	LLEESIQT	0.4514	0.8496	0.9727	0.391	1.0151	0.02235	
A15	333	FAMGVATTI	0.612	0.6652	0.98	0.7	0.9	0.09	
A24	321	KFAPGGYPL	0.2589	0.5513	0.9179	1.256	0.7518	0.05684	
B7	323	APGGYPLLW	0.3496	0.6745	0.9651	0.456	0.8421	0.01522	
B7	327	YPLLWSFAM	0.7282	1.4048	0.945	-0.032	1.545	0.16687	
B44	302	REIGPRAPY	0.2587	0.6411	0.9498	3.05	0.9361	0.14176	
Phosphoprotein									
A2	360	AQPPYHWSI	0.4199	0.626	0.9738	0.6	0.8021	0.10237	AQPPYHWSI
A24	360	AQPPYHWSI	0.3959	0.8429	0.9738	0.6	1.019	0.10237	
B44	360	AQPPYHWSI	0.258	0.6393	0.9738	0.6	0.8154	0.10237	
A3	665	KTLIRTHIK	0.6767	1.2736	0.9589	0.577	1.4463	0.32232	KTLIRTHIKDRELSELIGYLNK
B7	673	KDRELSEL	0.3868	0.7463	0.5517	0.812	0.8697	0.07435	
B44	679	SELIGYLNK	0.2388	0.5918	0.955	0.532	0.7617	0.1467	

3. Results and discussion

3.1. Selection of antigenic proteome of Nipah virus

All the essential proteins were retrieved from NCBI and checked for their antigenicity using the VaxiJen server which provided the antigenic score for each protein. For viruses, the VaxiJen score threshold is 0.4, i.e. proteins having a score higher than 0.4 are considered antigenic while <0.4 are non-antigenic in nature. Upon analysis of the evaluated proteins of the Nipah Virus, VaxiJen score was above 0.4 for all (Table 1).

The L protein was excluded from our analysis due to the involvement of RNA polymerase in replication. Therefore, the rest five antigenic proteins were taken into consideration for CTL, HTL, and B-cell epitope prediction using various immunoinformatics tools and servers. The schematic representation of the procedure followed for the prediction is shown in Figure 1.

3.2. Selection of major histocompatibility complex covering maximal world population

As the genes of MHCs are highly polymorphic and their expression profiles depend on the geographical location and ethnicity, for a vaccine to cover the entire world population, it must embed epitopes for the set of MHC class I/II that are present in the maximal population. To obtain the list of MHC class I and II complexes, the population coverage tool available at the immune epitope database (IEDB) server was employed. Various sets of MHC-I and MHC-II restricted alleles were fed in the server and their population coverage was observed.

We received six MHC class I supertypes namely HLA-A2, HLA-A3, HLA-A15, HLA-A24, HLA-B7 and HLA-B44 and ten MHC class II supertypes, HLA-DRB1*15:01, HLA-DRB1*15:02, HLA-DRB1*03:01, HLA-DRB4*01:01, HLA-DRB1*07:01, HLA-DRB5*01:01, HLA-DRB3*01:01, HLA-DRB1*01:01, HLA-DQA1*05:01/DQB1*05:02 and HLA-DPA1*01:03/DPB1*02:01 respectively that covers 96.21% of the world population.

Table 3. List of MHC-II allele epitopes for the Nipah virus protein with their IFN epitope prediction and the detailed information including the SMM align score, SMM align percentile rank, SMM align IC₅₀ value NN align score, NN align IC₅₀ value, NN align percentile rank, etc.

MHC II Allele	Start	End	Peptide	Method used	Percentile rank	SMM align score	SMM align IC ₅₀ (nM)	SMM align percentile rank	NN align score	NN align IC ₅₀ (nM)	NN align percentile rank	Consensus
HLA-DRB1*15:01	266	280	IYVDSLSSYYIIVRV	Consensus (smm/mn/sturniolo)	0.51	YVDLSSYYI	40	0.3	IYVDSLSSYY	11.1	0.51	IYVDSLSSYYIIVRVY
HLA-DRB1*15:01	267	281	IYVDSLSSYYIIVRVY	Consensus (smm/mn/sturniolo)	1.29	YVDLSSYYI	101	1.29	IYVDSLSSYY	14.4	0.85	
HLA-DRB1*15:02	266	280	IYVDSLSSYYIIVRV	Consensus (smm/mn/sturniolo)	0.435	IYVDSLSSYY	84.45	0.59	IYVDSLSSYY	1.4	0.90	
HLA-DRB3*01:01	452	466	VFYQASFSDTMKIF	Consensus (comb.lib./smm/mn)	0.23	YQASFSDWT	26	0.01	FSWDTMIKF	6.5	0.23	VFYQASFSDTMKIFG
HLA-DRB3*01:01	454	468	YQASFSDTMKFGD	Consensus (comb.lib./smm/mn)	0.01	FSWDTMIKF	26	0.01	FSWDTMIKF	6.8	0.25	
HLA-DRB3*01:01	453	467	FYQASFSDTMKFG	Consensus (comb.lib./smm/mn)	0.26	FSWDTMIKF	26	0.01	FSWDTMIKF	6.9	0.26	
HLA-DRB1*01:01	287	301	NNEFYVMLCAVSTVG	Consensus (comb.lib./smm/mn)	0.96	YYVLCAVST	8	0.96	YYVLCAVST	4.3	0.25	NNEFYVYVLCAVSTVG
HLA-DQA1*05:01/DQB1*05:02	224	238	MDEGYFAVSHLERIG	Consensus (comb.lib./smm/mn)	0.250	DEGYFAVSHLERIGS	25	0.408	DEGYFAVSHLERIGS	1.40		MDEGYFAVSHLERIGS
HLA-DQA1*05:01/DQB1*05:02	225	239	DEGYFAVSHLERIGS	Consensus (comb.lib./smm/mn)	0.275	DEGYFAVSHLERIGS	25	0.404	DEGYFAVSHLERIGS	1.60		
HLA-DPA1*01:03/DPB1*02:01	226	240	MDEGYFAVSHLERIGSCS	Consensus (comb.lib./smm/mn)	0.21	FAYSHLERI	3.6	0.21	FAYSHLERI	3.6	0.21	MDEGYFAVSHLERIGCS
HLA-DRB5*01:01	277	291	HIKINGVISKRIFFAQ	Consensus (smm/mn/sturniolo)	0.57	INGVISKRL	85	0.54	INGVISKRL	4.1	0.57	HIKINGVISKRIFFAQ
HLA-DRB5*01:01	276	290	LHIKINGVISKRIFLA	Consensus (smm/mn/sturniolo)	0.81	INGVISKRL	85	0.54	INGVISKRL	4.9	0.81	
HLA-DRB5*01:01	278	292	IKINGVISKRIFFAQM	Consensus (smm/mn/sturniolo)	1.04	INGVISKRL	85	0.54	INGVISKRL	5.6	1.04	
HLA-DRB1*07:01	285	299	NEFQSDLNTIKSLML	Consensus (comb.lib./smm/mn)	0.1	NEFQSDLNT	3	0.01	LNTIKSLML	3	0.1	NEFQSDLNTIKSLMLY
HLA-DRB1*07:01	286	300	EFGSDLNTIKSLMLL	Consensus (comb.lib./smm/mn)	0.11	LNTIKSLML	3	0.01	LNTIKSLML	3.1	0.11	
HLA-DRB1*07:01	287	301	FQSDLNTIKSLMLLY	Consensus (comb.lib./smm/mn)	0.24	LNTIKSLML	3	0.01	LNTIKSLML	3.8	0.24	
HLA-DRB4*01:01	216	230	EMRNLLSQSLSVRKF	Consensus (comb.lib./smm/mn)	0.91	MRNLLSQSL	163	0.91	MRNLLSQSL	8.9	0.21	-TEMRNLLSQSLSVRKFM
HLA-DRB4*01:01	217	231	MRNLLSQSLSVRKFM	Consensus (comb.lib./smm/mn)	1.14	MRNLLSQSL	191	1.14	RNLLSQSL	8.2	0.17	
HLA-DRB1*03:01	145	159	NGNVCLVSDAKMLSY	Consensus (smm/mn/sturniolo)	—	LVSDKMLS	37	0.01	LVSDKMLS	3.5	0.03	NNGNVCLVSDAKMLSY
HLA-DRB1*03:01	144	158	NNGNVCLVSDAKMLS	Consensus (smm/mn/sturniolo)	—	NNGNVCLVS	37	0.01	LVSDKMLS	4.7	0.07	

Thus, with high population coverage, these MHC supertypes were further used in our study. The MHC supertypes were also found to show high population coverage among the NPV risk population which mainly includes the South-east Asian countries (Figure S1).

3.3. MHC class I epitope prediction

The MHC class I epitopes activate the Cytotoxic T-cells, in turn, incite the adaptive immune system. Therefore prediction of MHC class I epitope is essential and here for our analysis, NetCTL 1.2 server was used for the prediction of MHC class I binders. NetCTL utilizes the artificial neural network (ANN) and weight matrix for 9 mer MHC class I epitope prediction. It integrates the propensity of proteasomal cleavage at the epitope's C terminal region, TAP transporting efficiency and MHC class I binding affinity and provides a score for each epitope. The prediction was done for the selected six MHC class I complexes, namely HLA-A2, HLA-A3, HLA-A15, HLA-A24, HLA-B7, and HLA-B44. For higher specificity (>98%) and selectivity, the NetCTL score >0.90 was used as the threshold. For each antigenic protein of the Nipah virus, the epitope(s) with score > 0.90 and covering the maximum number of MHC class I supertypes were selected.

Further, to check the immunogenicity and propensity of activating the Cytotoxic T-cells for the selected MHC class I binding epitopes, class I Immunogenicity tool available at the IEDEB server was exploited. Class I immunogenicity tool analyzes the 9 mer epitopes and provides a positive or a negative score. Higher the score depicts the greater probability of eliciting the immune response inside the host. Therefore, epitopes that provide only the positive score in the Class I immunogenicity analysis was taken into consideration and the negative ones were excluded.

Therefore, the epitopes that share the maximum number of MHC class I supertypes and provided the positive result in the Immunogenicity analysis were used for multi-epitope vaccine construct. The overlapping epitopes were merged and used as one. In the analysis, we received one epitope each from Glycoprotein, Nucleocapsid protein, Matrix protein, and Fusion protein while two from Phosphoprotein. (Table 2)

3.4. MHC class II epitope prediction

The MHC class II epitopes are recognized by the Helper T-lymphocytes (HTL/Th) cells which leads to activation of the humoral immune system. Therefore, to include the epitopes having the tendency to bind to MHC class II complex, 15 mer HTL specific epitopes were predicted by using the IEDEB MHC II epitope binding prediction tool. IEDEB MHC II binding prediction tool uses various algorithms including neural network (NN), artificial neural network (ANN), Sutniolo, and CombLib. Here, we utilized the integration of all these four algorithms for the prediction of HTL epitopes. The resultant epitopes were filtered based on IC₅₀ value which should be <50 nM and subsequently by percentile ranks. Epitope analysis was performed for the selected ten MHC II complexes

Table 4. List of linear B-cell epitopes with their location and score by using the BCPRED server.

Protein	Position	Epitope	Score
Fusion Protein	401	ISQSGEQTLLMIDNTTCPTA	0.987
Glycoprotein	268	TNVWTPPNPNTVYHCSAVN	0.999
Matrix Protein	71	VEDVERTPETGKRKKIRTIA	0.998
Nucleocapsid	485	AKAAKEAASSNATDDPAISN	0.997
Phosphoprotein	304	TDVPGAGPKDSAVKEEPQK	1

and the epitopes with least IC₅₀ and highest percentile rank were selected for each MHC-II complexes.

From the variety of cytokines secreted by HTLs, Interferon gamma (IFN- γ) are the major ones that help in generation of antiviral immunity, enhancing antigen presentation on APCs and subsequent macrophage activation activates innate immune system and manages Th1/Th2 balance, cellular proliferation, and apoptosis, thus leading to induction of multiple arrays of immune response (Billiau, 1996; Boehm, Klamp, Groot, & Howard, 1997). Thus, the filtered HTLs from IEDEB analysis were further analyzed for their ability to induce IFN- γ production. For this, the epitopes were mined by using Support vector machine algorithm available at the IFNepitope server. Based on the prediction score, the IFNepitope server predicts the epitopes for the propensity of inducing INF γ formation. The HTL epitopes that showed a positive score in the IFNepitope server were taken for multi-epitope vaccine construct formation. Thus, upon analysis, we received best epitopes for HLA-DRB1*15:01 and HLA-DRB1*15:02 for Fusion protein, HLA-DRB1:03:01 for Phosphoprotein, HLA-DRB4*01:01 and HLA-DRB1*07:01 for Nucleocapsid proteins, HLA-DRB5*01:01 for Matrix protein and HLA-DRB3*01:01, HLA-DRB1*01:01, HLA-DQA1*05:01/DQB1*05:02 and HLA-DPA1*01:03/DPB1*02:01 for Glycoprotein of the Nipah virus (Table 3).

3.5 B-cell epitope prediction

B-lymphocytes are the integral part of the humoral immune system that generate diversified but pathogen specific antibodies leading to antigen neutralization and viral load clearance. To include the epitopes having the propensity of activating the B-cells in the vaccine construct, the antigenic proteome was analyzed by using the BCPRED server. The best epitope from each antigenic protein with the highest score was used for the vaccine construction (Table 4).

3.6. Molecular interaction analysis of CTL and HTL epitopes with the MHC complex

Major histocompatibility complex class I and class II share a common epitope binding groove where epitope interacts with the T-Lymphocytes and thereby are presented to them. For analyzing the interaction of the selected CTL and HTL epitopes with the epitope binding groove of the MHC class I and II complex, molecular docking analysis was performed by using the ClusPro server and the results were visualized by using the PyMol. Docking analysis in the ClusPro server was performed in three steps namely, 1) generation of billions of conformers and then performing rigid body based docking analysis, 2) RMSD based clustering of the docked

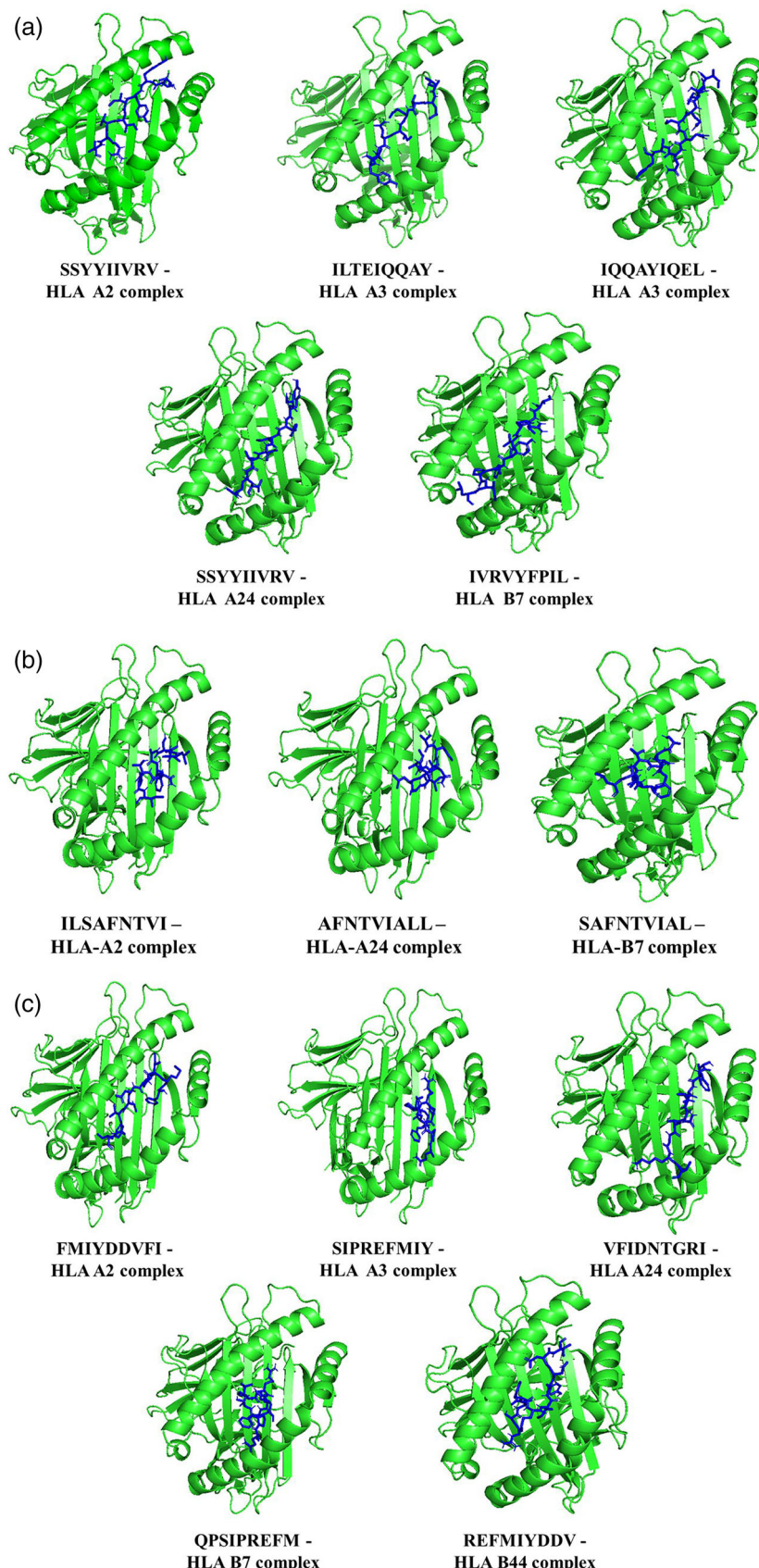
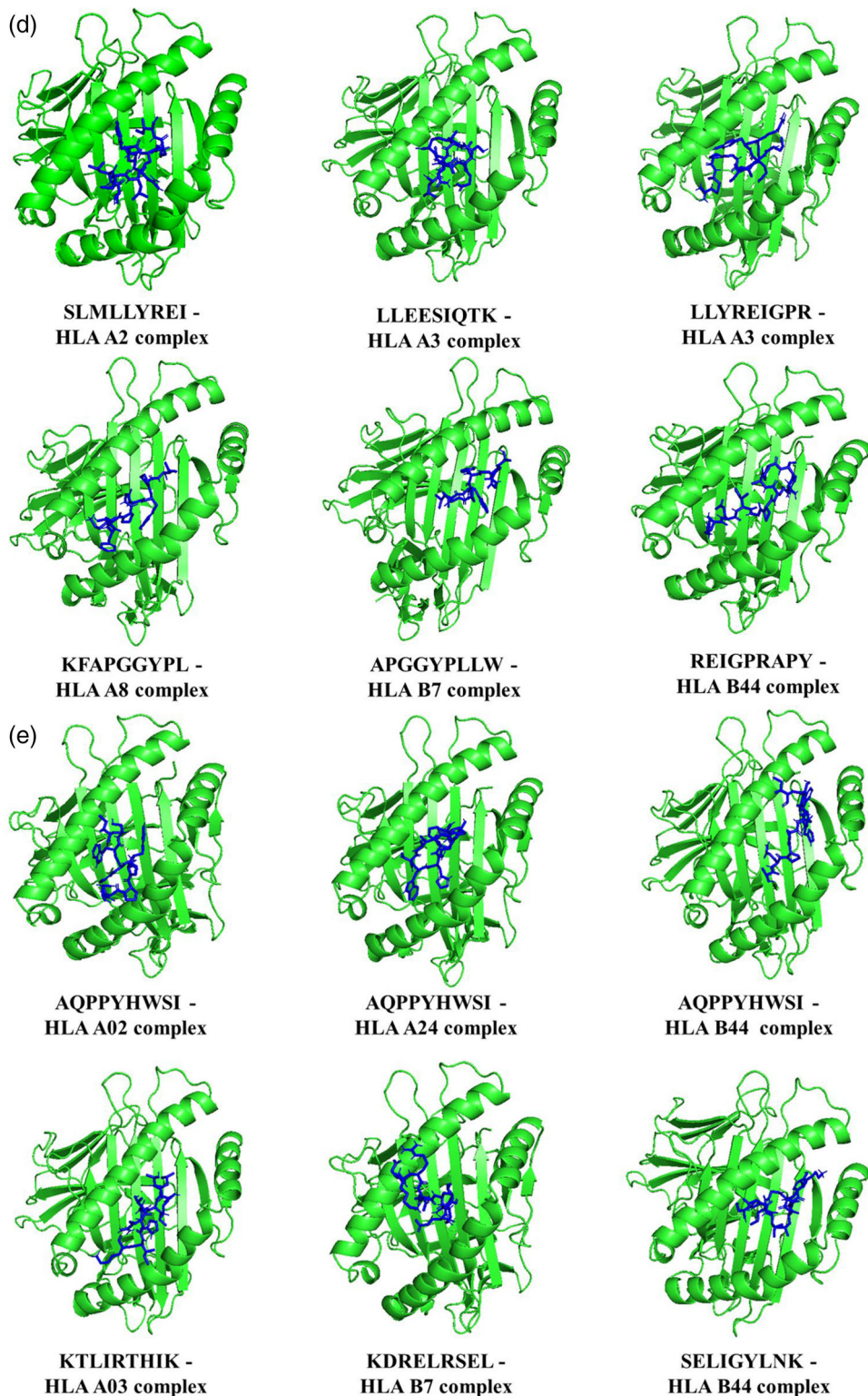


Figure 2. a: Molecular interaction of Fusion protein epitopes with different HLA gene. b: Molecular interaction of Glycoprotein epitopes with different HLA gene. c: Molecular interaction of Matrix protein epitopes with different HLA gene. d: Molecular interaction of Nucleocapsid protein epitopes with different HLA gene. e: Molecular interaction of Phosphoprotein epitopes with different HLA gene.

**Figure 2.** Continued.

complex based on the lowest energy model and 3) finally energy minimization of the refined docked complex. MHC I/II complexes were used as receptors, while epitopes were used as ligands in the docking process. The epitope-HLA interaction analysis revealed the interaction of CTL and HTL epitopes in the binding cleft of the respective MHC supertype complexes (Figures 2a-e, 3).

3.7. Designing of the Nipah multi-valent vaccine construct

The multi-valent vaccine construct was designed as per the illustrated **Figure 4**. The selected CTL, HTL and B-cell epitopes were linked together in the same order by utilizing AAY, GGGGS and KK linkers respectively. For enhancing the immune response, three adjuvants were also added in the

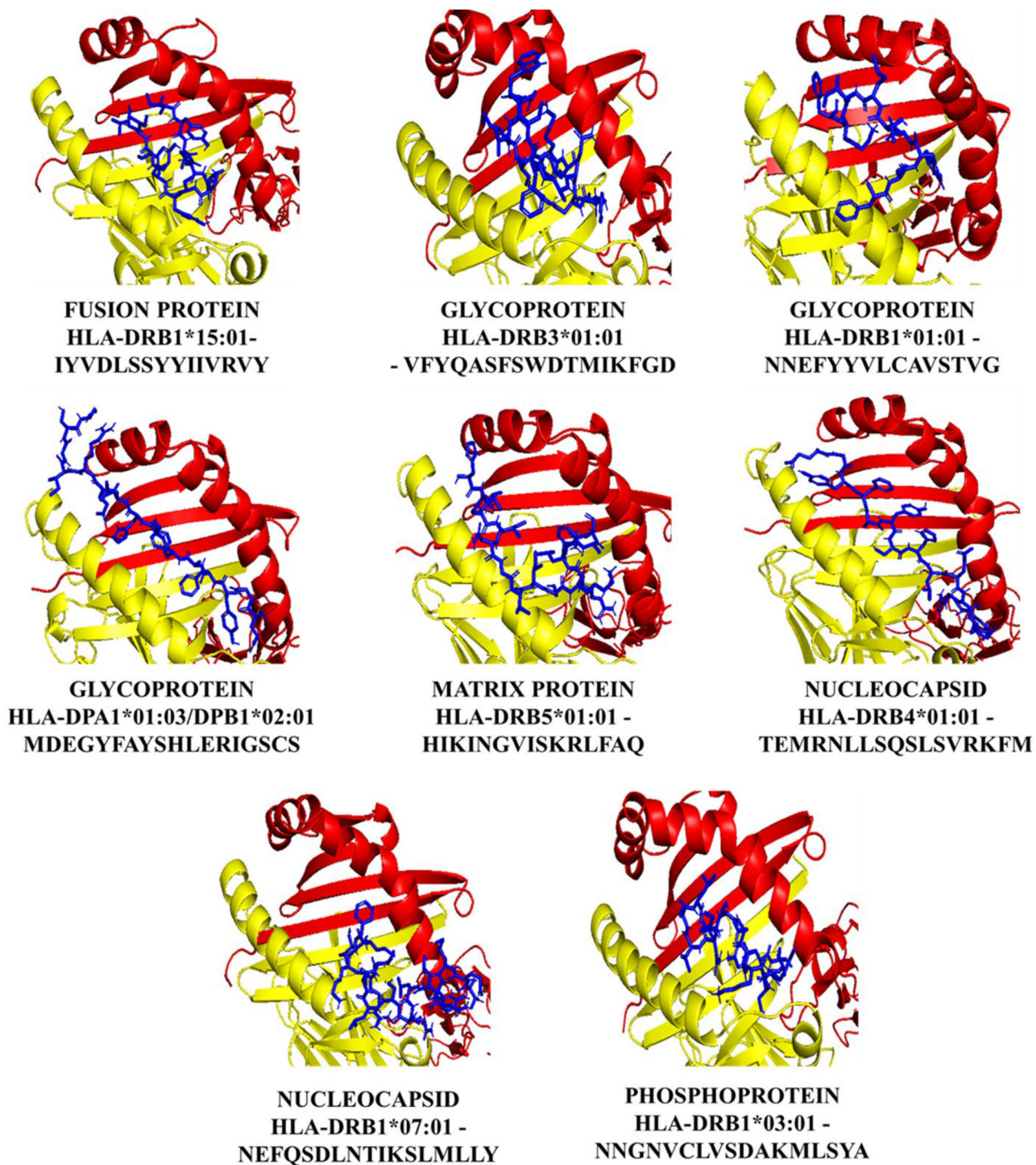


Figure 3. Molecular interaction of HTLs with MHC II complexes for the antigenic proteins.

vaccine construct. β -defensins, cationic antimicrobial peptides assist in the generation of resistance on the epithelial surface against the microbial colonization. As well, β -defensin administration along with the antigens is reported to enhance the humoral and cellular mediated immune response by the production of respective cytokines. Thus, β -defensins act as adjuvants for the generation of an effective immune response (Oppenheim et al., 2003). Therefore, a β -defensin 3 (Uniprot ID – Q5U7J2) sequence was added at the N-terminal region of the vaccine construct.

Similarly, to enhance the CD4 mediated Helper T-Lymphocyte immunogenic response, a universal CD4 memory T-cell peptide (TpD) derived from tetanus and diphtheria toxoids having an internal cathepsin cleavage site was added to the vaccine construct between CTL and HTL epitopes. TpD peptide has a high propensity to interact with the diversified MHC class II alleles of the human population (Fraser et al., 2014). Additionally, for the effective adsorption from the intestinal gut barrier, an additional peptide motif “CTGKSC” was added to the C-terminal region of the vaccine construct. This peptide interacts with the M-cells of the intestine that

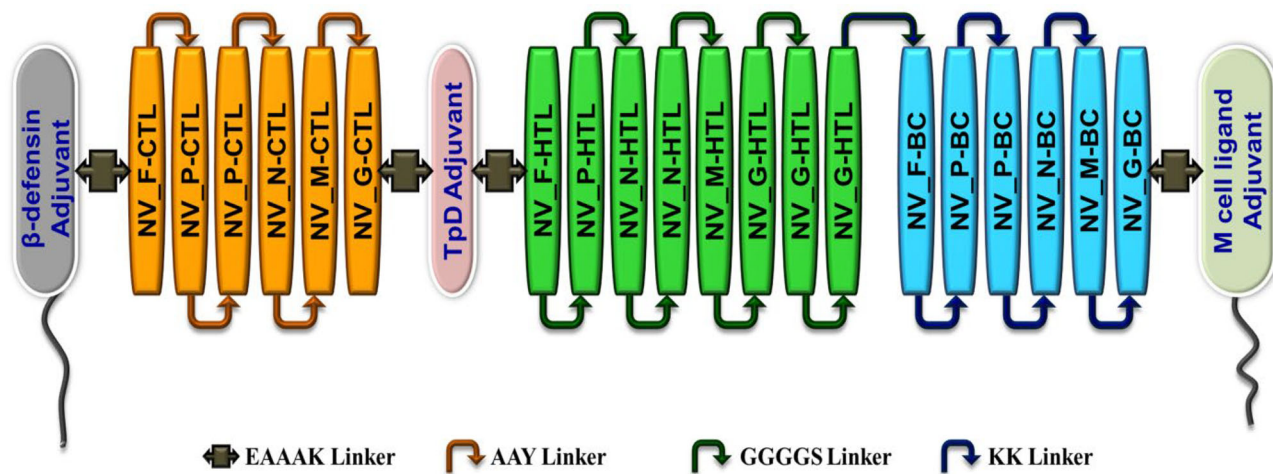


Figure 4. Schematic representation of the multi-epitope vaccine construct. The vaccine construct (562 aa) composed of three adjuvants namely β -defensin, Universal T helper adjuvant (TpD) and M-cell ligand attached by EAAAK linkers with the epitopes. Cytotoxic T-cell epitopes (orange) were linked together by AAY linker, Helper T-cell epitopes; HTLs (green) by GGGGS linker and B-cell epitopes (sky blue) by KK linkers.

Table 5. Table showing the different properties of the multivalent epitope vaccine designed.

Properties of the multivalent epitope vaccine construct	Tools used	Results
Bio-physical properties	ProtParam	Number of amino-acids: 562 Molecular weight: 61.27466 kDa Theoretical pI: 9.12 Estimated half-life: 30 hours (mammalian reticulocytes, in vitro); >20 hours (yeast, in vivo); >10 hours (Escherichia coli, in vivo). Instability index: 39.00 (stable) Aliphatic index: 88.42 Grand average of hydropathicity (GRAVY): -0.012
Allergenic properties	AllerTOP AlgPred	Probable non-allergen Non-allergen in nature
Antigenic properties	VaxiJen Server AntigenPro	Score: 0.4025 (Probable ANTIGEN; Threshold: 0.4) Predicted Probability of Antigenicity: 0.74781

helps in the efficient transportation of antigens from the lumen to the immune system cells (Fievez et al., 2010). Thus, β -defensin and TpD peptides help in the enhancement of innate and adaptive immune response while M-cell ligand mediates the active adsorption and transportation of the vaccine to the immune system. For the effective domain separation and expression of these three adjuvants, they were separated from the epitopes by EAAAK linkers (Arai, Ueda, Kitayama, Kamiya, & Nagamune, 2001). To enhance the multi-subunit vaccine recognition, CTL and HTL epitopes were linked together by using AAY and GGGGS linkers respectively. KK linkers were utilized for separate B-cell epitopes. These bi-lysine linkers help in maintaining the independent immunogenic properties of the epitopes. By combining CTLs, HTLs, B-cell epitopes and three adjuvants, a vaccine peptide of 562 amino acids was constructed. This peptide sequence was used as a multi-subunit vaccine construct and utilized for secondary and tertiary structure prediction.

3.8. Antigenicity and allergenicity analysis of the vaccine construct

To elicit maximum immunogenicity and minimum off-target effects and allergic response, a peptide must possess the antigenic and non-allergenic properties. For antigenic analysis,

VaxiJen and AntigenPro tool at the SCRATCH server was utilized. Both the servers predicted the antigenic nature of the multi-subunit vaccine. To avoid any allergic immune response generated by the hypersensitivity of the peptides with the IgE antibodies, the allergenicity analysis was performed by using AlgPred and AllerTop tools. The AlgPred analysis showed the absence of experimentally proven IgE epitopes thus showing the non-allergenic nature of the predicted epitopes. The AllerTop prediction of the vaccine construct was in line with the AlgPred tool (summarized in Table 5).

3.9. Analysis of physicochemical properties of multi-epitope vaccine construct

For a peptide to act as an efficient vaccine, it should embed various physicochemical properties. One of these physicochemical properties is molecular weight. The molecular weight is inversely proportional to the half-life of the peptide inside the body but is directly proportional to the lymph node exposure (Wu et al., 2012). Therefore, for maximal half-life and lymph node exposure for the active immune response generation, peptides with greater than 50 kDa are considered good vaccine options. Moreover, hydrophobicity and hydrophilicity greatly affect the effectiveness of the vaccine construct. Thus, to evaluate the physicochemical properties of the Nipah vaccine

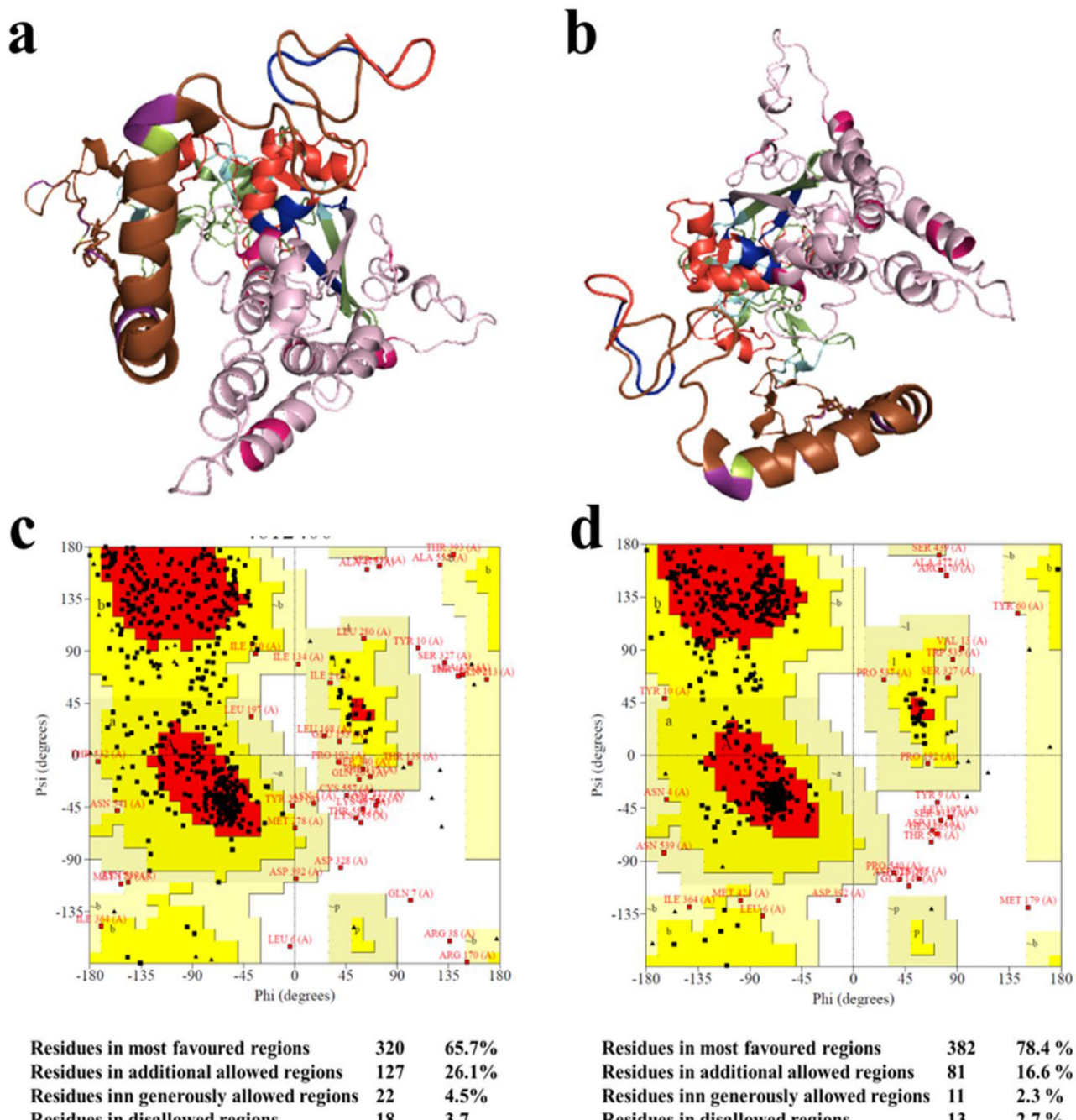


Figure 5. Molecular modeling of the multi-epitope vaccine construct. (a-b) Tertiary structures of the Nipah virus multi-epitope vaccine construct. Adjuvants are represented by red, EAAAY linker by blue, AAY by pink, GGGGS by cyan, KK by purple, B-cell epitopes by brown, HTLs epitopes by smudge and CTL epitopes by light-pink color. Ramachandran plot depicting the residues in the favoured, allowed and disallowed region for the vaccine construct before structure refinement (c) and after structure refinement (d).

construct, the ProtParam tool available at the Expasy server was utilized. The molecular weight was predicted to be 61.27 kDa with a predicted half-life of 30 h in mammalian reticulocytes. ProtParam classified the vaccine construct as stable in nature with the instability index of only 39 (summarized in Table 5).

3.10. Structure prediction and validation of multi-subunit vaccine construct

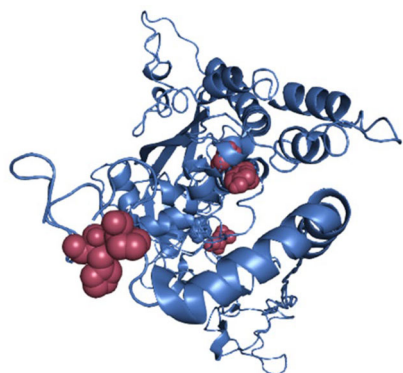
For analyzing the stability of the vaccine construct in the real environment, the 562 aa peptide sequence was used for the

prediction of secondary and tertiary structure prediction of the vaccine construct. For secondary structure prediction, the PSIPRED server was utilized. PSIPRED predicts the secondary structure by aligning the input sequence using PSI-PRED and subsequently classifies the sequences depending on the propensity of forming alpha-helix, beta-sheets, and loops/turns. The predicted secondary structure of the Nipah virus subunit vaccine is given in Figure S2.

For tertiary structure prediction, automated multi-template based threading algorithm available at I-TASSER server was utilized. Based on C-score generated by the I-TASSER

which depends upon the sequence similarity with the templates used, the best model with the highest C-score was selected and utilized for further analysis (Table S3). The obtained structure was further validated by constructing the Ramachandran plot using the RAMPAGE tool. The Ramachandran plot depicted 73.4% of residues lie in the most favoured region while 18% in the allowed region. 8.8% of the residues were in the outlier region of the

Ramachandran plot. Therefore, to enhance the stability of the predicted structure and to increase the number of residues in the favourable region, the structure was refined by using GalaxyRefine. The refinement of the GalaxyRefine server is performed by employing the molecular dynamics simulations and repeated structural perturbations in the preliminary structure were submitted that generated five refined models (Table S4). Ramachandran plot analysis was performed on all the five refined structures and model 3 on the basis of higher number of residues in the favourable region (87.1% in favoured and 9.8% in the allowed region with only 3% in the outlier region) was selected as the best model of the Nipah vaccine construct (Figure 5).



Res1 Chain	Res1 Seq #	Res1 AA	Res2 Chain	Res2 Seq #	Res2 AA	Chi3	Energy
A	538	PRO	A	545	HIS	-82.65	0.32
A	202	ALA	A	223	TYR	-80.87	1.12
A	19	ALA	A	346	LEU	96.48	1.41

Figure 6. Disulfide engineering: Representation of the residues (purple) in the tertiary structure of the vaccine construct and the details of the residues that were used for disulfide engineering.

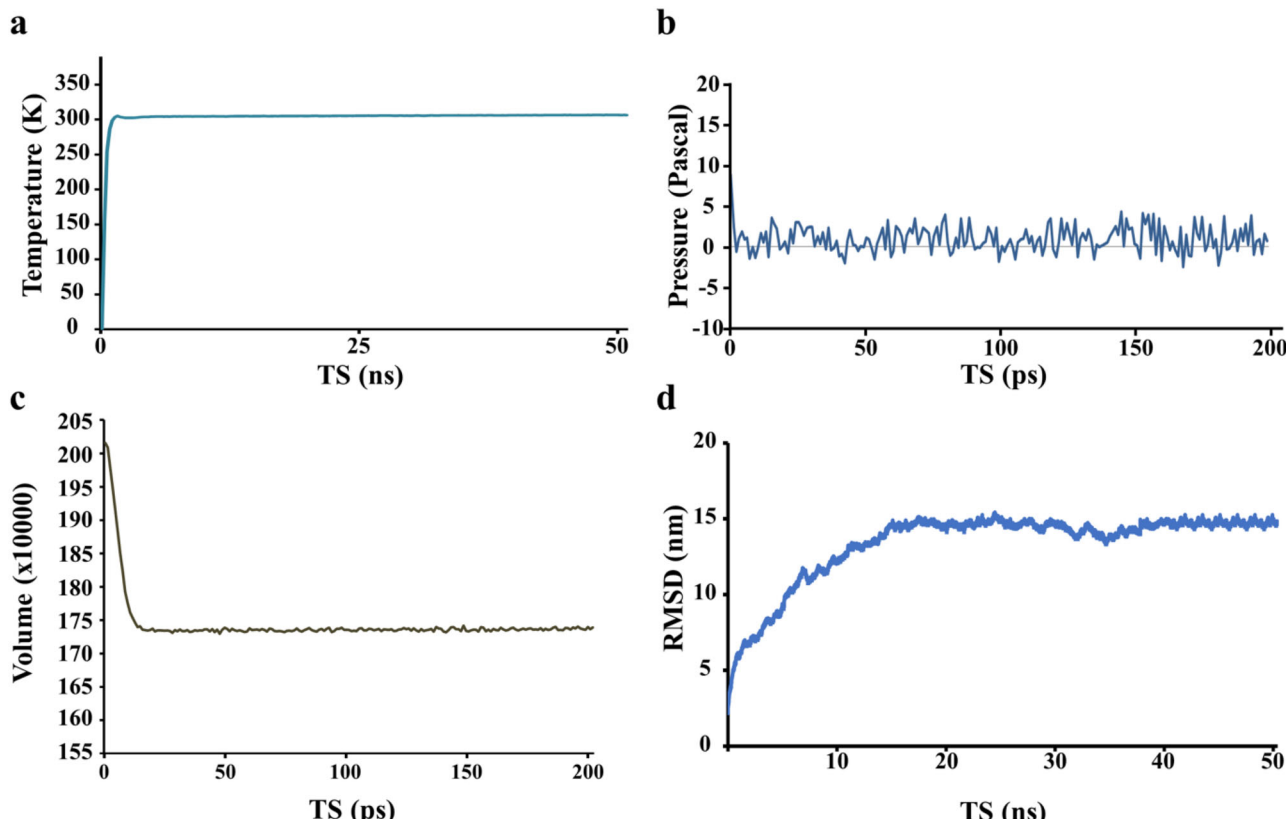


Figure 7. Molecular Dynamic analysis of the Multi-epitope vaccine construct: (a) Temperature vs TS curve for 50 ns molecular dynamic simulation depicting the constant temperature of ~310 K throughout the simulation analysis. (b) NPT curve drawn between Pressure and Time Step(TS) depicting the constant pressure for 200 ps. (c) NVT simulation analysis depicting the constant volume for 200 ps. (d) RMSD analysis for 50 ns molecular dynamic simulation analysis depicting the stability of the multi-epitope vaccine construct.

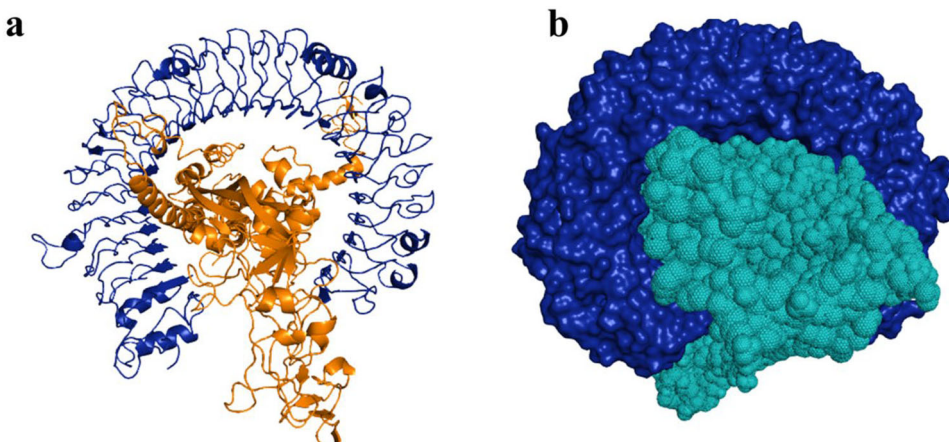


Figure 8. Molecular interaction of multi-epitope vaccine construct with TLR3 of humans. (a) Cartoon representation of TLR3 (blue) and vaccine construct (brown) (b) Surface representation of TLR3 (blue) with sphere representation of the vaccine construct (marine blue).

and 223 TYR, and 19 ALA and 346 LEU) were selected for disulfide engineering (Figure 6, Table S5).

Furthermore, to check the effect of these three constructed novel disulfide bonds on the stability of the vaccine construct, the ERIS tool was utilized. Eris is used for analyzing the change in protein stability (in terms of change in free energy, $\Delta\Delta G$) that is induced by mutation in the native structure. $\Delta\Delta G < 0$ showed the stabilizing effect of the mutation and vice-versa. Upon analysis, $\Delta\Delta G$ due to the creation of three disulfide bonds was calculated to be -31.44 kcal/mol thus depicting the stabilization effect of disulfide engineering on the vaccine construct (Yin et al., 2007).

3.12. Molecular dynamics analysis of the multi-subunit vaccine construct

Biological functions of a vaccine depend upon its interaction with other molecules which further depend upon the macromolecular structure. To analyze the vaccine structure and its stability in biological conditions, molecular dynamics (MD) simulation analysis was performed by using NAMD. Initially, 10,000 steps of energy minimization were performed for the vaccine construct followed by subsequent heating of the system to 310 K. After that, 200 picosecond simulation was performed at constant pressure (NPT) followed by 50 ns dynamic analysis at constant volume (NVT). A 50 ns MD simulation using GROMACS forcefield was performed and trajectory analysis during this time course was analyzed at a constant temperature of 310 K. Trajectory analysis of the vaccine construct depicted that Root Mean Square Deviation (RMSD) became constant after 400 femtoseconds after which only minor changes were observed. This depicted the stable nature of multi-subunit vaccine construct (Figure 7). Total energy, kinetic and potential analysis of the vaccine construct in the water sphere with respect to time also depicted that the system came at equilibrium after 400 femtoseconds (Figure S6).

3.13. Molecular interaction of the vaccine construct with the human TLR-3

Toll-like receptor proteins are crucial for pathogen recognition and innate immune system activation and are one for

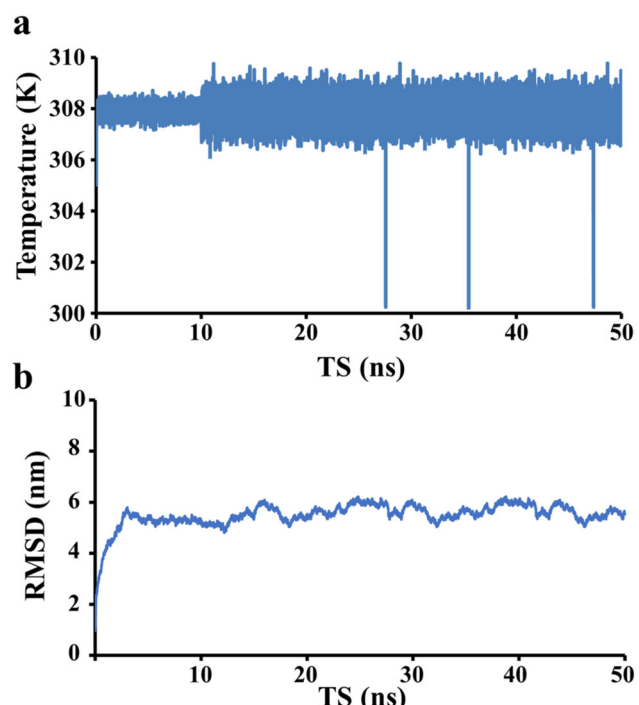


Figure 9. Molecular dynamic analysis of the TLR3-vaccine construct complex. (a) Temperature vs Time steps curve for 50 ns. The temperature remained constant throughout the simulation analysis. (b) RMSD curve obtained from the trajectory analysis of the 50 ns molecular dynamic simulation of the docked complex. The complex inside the water sphere remained constant after ~ 3 ns.

the preliminary receptors that sense the entry of foreign particles cascading the stimulation of various signaling pathways. TLR3 recognizes dsRNA of the viruses and induces the NF- κB cytokine production leading to the generation of host defense against viruses. Nipah virus combat with the host anti-viral defense by inhibiting the TLR3 signaling pathway (Shaw et al., 2005). Therefore, to analyze the molecular interaction of the vaccine construct with human TLR-3 complex, docking analysis was performed by using the ClusPro server where TLR3 was submitted as the receptor while the vaccine construct was used as ligand. The best docked complex was used for molecular dynamics analysis (Figure 8).

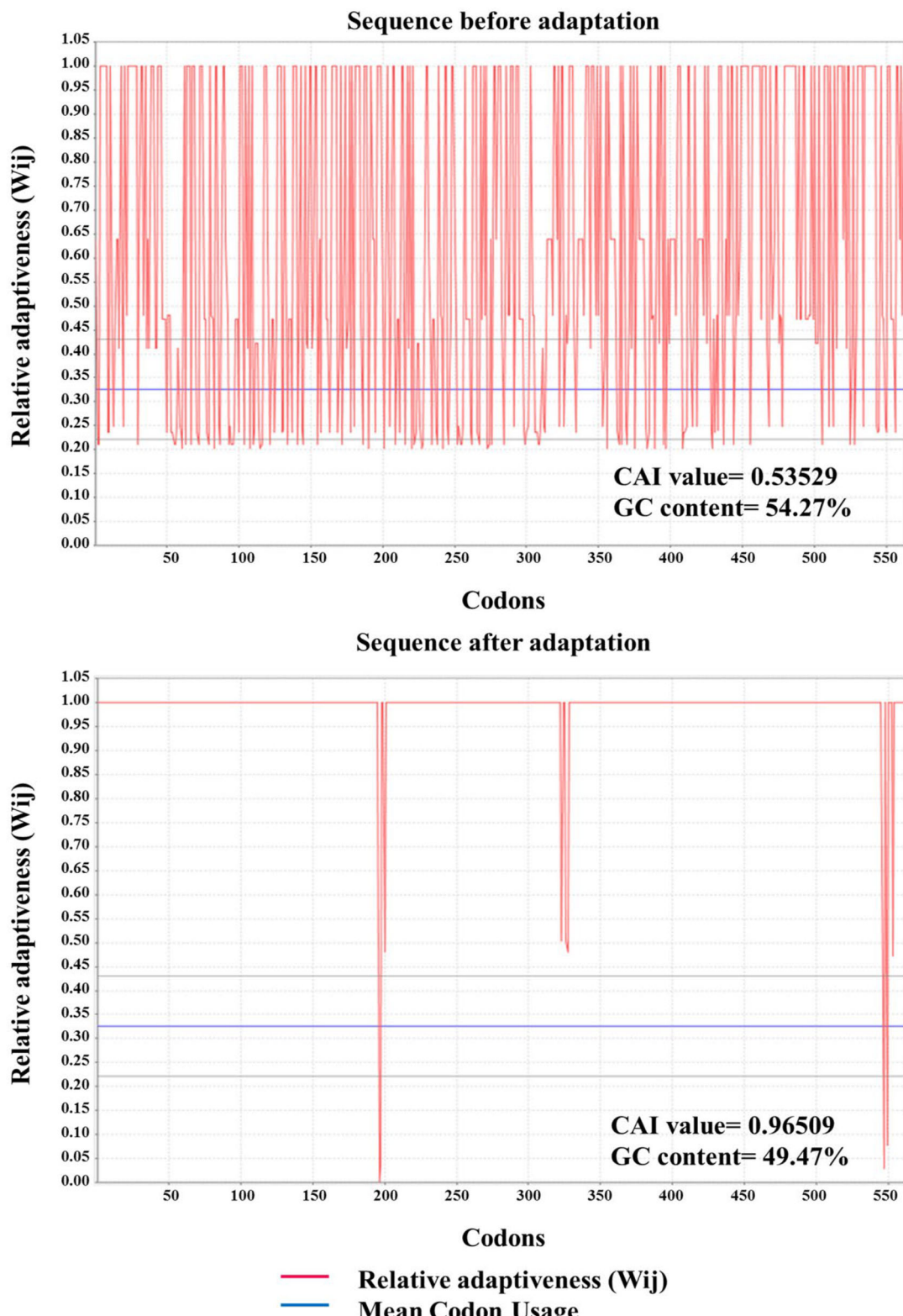


Figure 10. a: cDNA codon optimization. Graphical representation of the Codon adaption index (CAI-values) and GC content of the cDNA of the vaccine construct before adaptation (a) and after adaptation (b). b: *In silico cloning* of the vaccine construct. The cDNA of the vaccine construct (green) was inserted at the upstream of the T7 promoter. The vaccine construct was tagged with 6X histidine tags at the 3' end of the cDNA.

3.14. Stabilization of the docked complex of vaccine construct and TLR-3

Molecular dynamics simulation can be considered a great way of analyzing the stability of the docked complex. 50 ns

simulation analysis of the Vaccine construct-TLR3 complex depicted the stabilization of the complex after ~3 ns after which, RMSD remained constant (Figure 9). Change in total energy, kinetic and potential energy of the docked complex system is represented in Figure S7.

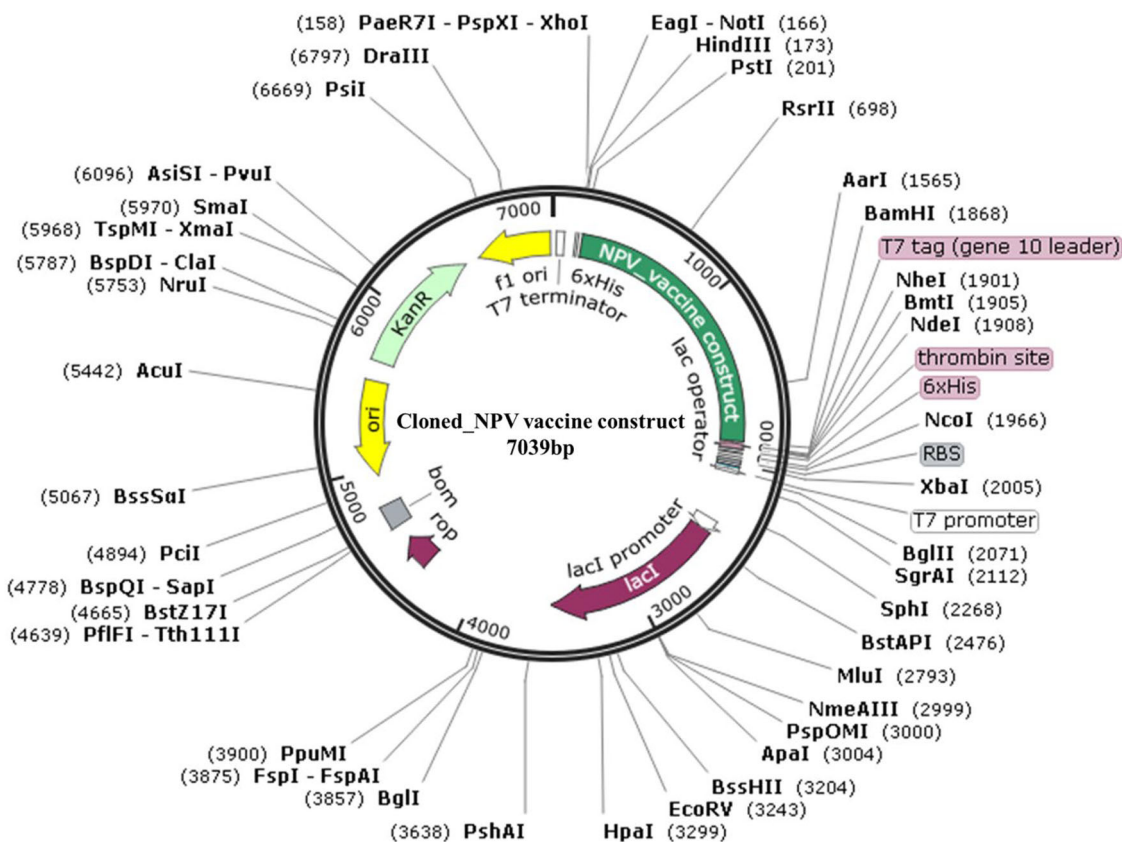


Figure 10. Continued

3.15 cDNA construction and *in silico* cloning of the vaccine construct

For the efficient expression and purification of the multi-subunit vaccine, a proper expression system with codons optimally selected as per the expression host is a pre-requisite. For this, the primary step is to synthesize cDNA for the vaccine construct. Reverse translate tool that uses the amino acid sequence to generate a cDNA was utilized for this purpose. Reverse translation of the Nipah virus multi-epitope vaccine resulted in the generation of 1686 bp cDNA construct with 54.27% GC content. The selection of codons for specific amino acids during translation varies with the host organism. This codon usage by the organism is usually represented by the Codon Adaptation Index (CAI) that varies from 0 to 1, where 0 depicts that the specific codon is not utilized by the host and 1 represents the maximal usage of the codon depicting the optimal codon usage by the organism. For the *Escherichia coli* K12 strain, the CAI value of the vaccine construct cDNA was found to be 0.53. For further codon optimization of the cDNA as per the *Escherichia coli* K12 strain, Java Codon Adaptation Tool (JCAT) was explored. As well for optimal full-length protein expression, the mRNA must be free of any internal rho-independent termination (*ter*) sites. Furthermore, for the insertion of the cDNA in the expression vector, the cDNA construct was analyzed for the presence of two most frequently used restriction enzymes, *BamH*I and *Hind*III. The *ter* sites, *BamH*I sites, and *Hind*III sites if any were replaced as per the codon usage by using

the JCAT tool. The resultant adapted cDNA had a CAI index of 0.96 and a 49.46% GC content (Figure 10a).

The adapted cDNA was then inserted in pET28(a)+ expression vector by utilizing *BamH*I and *Hind*III restriction enzymes in the SnapGene tool (Figure 10b). This *in silico* cloning leads to the generation of 7039 bp expression vector that can be used for optimal expression of the multi-subunit vaccine construct in the *Escherichia coli* K12 expression system. For efficient purification of the vaccine construct, 6X His tag was inserted at the C-terminal region of the cDNA.

4. Conclusion

Nipah virus is one of the most pernicious zoonotic viruses re-emerging in certain pockets of the world. With no licensed vaccine or drug against this virus, the situation during an outbreak gets worsened. The case-fatality rate reaching upto 91% and having long-term neurological sequelae even after survival from the disease urge the need for the development of an effective vaccine against this virus. Here we have designed a multivalent epitope-based against the Nipah using different online-available tools and servers. This study puts forward an effective vaccine candidate combining the best suitable epitope for all the five Nipah viral genes (except the polymerase L gene) and the detailed analysis of this vaccine reveals the high propensity of the vaccine to elicit both innate and adaptive immunity in humans. Moreover, the results depict that the multi-peptide vaccine can easily be expressed in a typical bacterial system like

E.coli and thus can prove to be a highly efficacious prophylactic solution for the Nipah viral disease.

Acknowledgements

PM acknowledges the Ministry of Human Resource Development (MHRD), New Delhi and NJ to the Council of Scientific & Industrial Research (CSIR), New Delhi for their respective fellowships. We acknowledge Indian Institute of Technology, Indore for computational facilities.

Disclosure statement

The authors declare no competing interest.

Authors contribution

AK conceptualized the idea and did the critical analysis of the manuscript. PM and NJ together carried on the immune-informatics analysis and drafted the manuscript.

ORCID

Prativa Majee  <http://orcid.org/0000-0001-6807-010X>
 Neha Jain  <http://orcid.org/0000-0003-4627-3349>
 Amit Kumar  <http://orcid.org/0000-0002-5913-4308>

References

- Ahmad, K. (2000). Malaysia culls pigs as Nipah virus strikes again. *The Lancet*, 356(9225), 230. doi:[10.1016/S0140-6736\(05\)74483-4](https://doi.org/10.1016/S0140-6736(05)74483-4)
- Ang, B. S. P., Lim, T. C. C., & Wang, L. (2018). Nipah Virus Infection. *Journal of Clinical Microbiology*, 56(6), e01875-01817. doi:[10.1128/JCM.01875-17](https://doi.org/10.1128/JCM.01875-17)
- Arai, R., Ueda, H., Kitayama, A., Kamiya, N., & Nagamune, T. (2001). Design of the linkers which effectively separate domains of a bifunctional fusion protein. *Protein Engineering Design and Selection*, 14(8), 529–532. doi:[10.1093/protein/14.8.529](https://doi.org/10.1093/protein/14.8.529)
- Bappy, S. S., Sultana, S., Adhikari, J., Mahmud, S., Khan, M. A., Kaderi Kibria, K. M., ... Shibly, A. Z. (2020). Extensive Immunoinformatics study for the prediction of novel peptide-based epitope vaccine with docking confirmation against Envelope protein of Chikungunya virus: A Computational Biology Approach. *Journal of Biomolecular Structure and Dynamics*, 1–30. doi:[10.1080/07391102.2020.1726815](https://doi.org/10.1080/07391102.2020.1726815)
- Bhattacharya, M., Malick, R. C., Mondal, N., Patra, P., Pal, B. B., Patra, B. C., & Kumar Das, B. (2020). Computational characterization of epitopic region within the outer membrane protein candidate in *Flavobacterium columnare* for vaccine development. *Journal of Biomolecular Structure and Dynamics*, 38(2), 450–459. doi:[10.1080/07391102.2019.1580222](https://doi.org/10.1080/07391102.2019.1580222)
- Billiau, A. (1996). Interferon-gamma: Biology and role in pathogenesis. *Advances in Immunology*, 62, 61–130. doi:[10.1016/s0065-2776\(08\)60428-9](https://doi.org/10.1016/s0065-2776(08)60428-9)
- Boehm, U., Klamp, T., Groot, M., & Howard, J. C. (1997). Cellular responses to interferon-gamma. *Annual Review of Immunology*, 15(1), 749–795. doi:[10.1146/annurev.immunol.15.1.749](https://doi.org/10.1146/annurev.immunol.15.1.749)
- Bossart, K., Rockx, B., Feldmann, F., Brining, D., Scott, D., LaCasse, R., ... Hickey, A. (2012). A Hendra virus G glycoprotein subunit vaccine protects African green monkeys from Nipah virus challenge. *Science Translational Medicine*, 4, 146ra107. doi:[10.1126/scitranslmed.3004241](https://doi.org/10.1126/scitranslmed.3004241)
- Bui, H. H., Sidney, J., Dinh, K., Southwood, S., Newman, M. J., & Sette, A. (2006). Predicting population coverage of T-cell epitope-based diagnostics and vaccines. *BMC Bioinformatics*, 7(1), 153. doi:[10.1186/1471-2105-7-153](https://doi.org/10.1186/1471-2105-7-153)
- Calis, J. J. A., Maybeno, M., Greenbaum, J. A., Weiskopf, D., De Silva, A. D., Sette, A., ... Peters, B. (2013). Properties of MHC Class I Presented Peptides That Enhance Immunogenicity. *PLOS Computational Biology*, 9(10), e1003266. doi:[10.1371/journal.pcbi.1003266](https://doi.org/10.1371/journal.pcbi.1003266)
- Chua, K. B., Bellini, W. J., Rota, P. A., Harcourt, B. H., Tamin, A., Lam, S. K., ... Mahy, B. W. J. (2000). Nipah virus: A recently emergent deadly paramyxovirus. *Science*, 288(5470), 1432–1435. doi:[10.1126/science.288.5470.1432](https://doi.org/10.1126/science.288.5470.1432)
- Clayton, B. A. (2017). Nipah virus: Transmission of a zoonotic paramyxovirus. *Current Opinion in Virology*, 22, 97–104. doi:[10.1016/j.coviro.2016.12.003](https://doi.org/10.1016/j.coviro.2016.12.003)
- Craig, D. B., & Dombkowski, A. A. (2013). Disulfide by Design 2.0: A web-based tool for disulfide engineering in proteins. *BMC Bioinformatics*, 14(1), 346. doi:[10.1186/1471-2105-14-346](https://doi.org/10.1186/1471-2105-14-346)
- Dhanda, S. K., Vir, P., & Raghava, G. P. (2013). Designing of interferon-gamma inducing MHC class-II binders. *Biology Direct*, 8(1), 30. doi:[10.1186/1745-6150-8-30](https://doi.org/10.1186/1745-6150-8-30)
- Dimitrov, I., Bangov, I., Flower, D. R., & Doytchinova, I. (2014). AllerTOP v.2—a server for in silico prediction of allergens. *Journal of Molecular Modeling*, 20(6), 2278. doi:[10.1007/s00894-014-2278-5](https://doi.org/10.1007/s00894-014-2278-5)
- Dombkowski, A. A., Sultana, K. Z., & Craig, D. B. (2014). Protein disulfide engineering. *FEBS Letters*, 588(2), 206–212. doi:[10.1016/j.febslet.2013.11.024](https://doi.org/10.1016/j.febslet.2013.11.024)
- Dorost, H., Eslami, M., Negahdaripour, M., Ghoshoon, M. B., Gholami, A., Heidari, R., ... Ghasemi, Y. (2019). Vaccinomics approach for developing multi-epitope peptide pneumococcal vaccine. *Journal of Biomolecular Structure and Dynamics*, 37(13), 3524–3535. doi:[10.1080/07391102.2018.1519460](https://doi.org/10.1080/07391102.2018.1519460)
- Doytchinova, I. A., & Flower, D. R. (2007). VaxiJen: A server for prediction of protective antigens, tumour antigens and subunit vaccines. *BMC Bioinformatics*, 8(1), 4. doi:[10.1186/1471-2105-8-4](https://doi.org/10.1186/1471-2105-8-4)
- El-Manzalawy, Y., Dobbs, D., & Honavar, V. (2008). Predicting linear B-cell epitopes using string kernels. *Journal of Molecular Recognition*, 21(4), 243–255. doi:[10.1002/jmr.893](https://doi.org/10.1002/jmr.893)
- Fievez, V., Plapied, L., Plaideau, C., Legendre, D., Des Rieux, A., Pourcelle, V., ... Schneider, Y. J. (2010). In vitro identification of targeting ligands of human M cells by phage display. *International Journal of Pharmaceutics*, 394(1-2), 35–42. doi:[10.1016/j.ijpharm.2010.04.023](https://doi.org/10.1016/j.ijpharm.2010.04.023)
- Fraser, C. C., H. Altreuter, D., Ilyinskii, P., Pittet, L., LaMothe, R. A., Keegan, M., ... Kishimoto, T. K. (2014). Generation of a universal CD4 memory T cell recall peptide effective in humans, mice and non-human primates. *Vaccine*, 32(24), 2896–2903. doi:[10.1016/j.vaccine.2014.02.024](https://doi.org/10.1016/j.vaccine.2014.02.024)
- Germain, R. N. (1994). MHC-dependent antigen processing and peptide presentation: Providing ligands for T lymphocyte activation. *Cell*, 76(2), 287–299. doi:[10.1016/0092-8674\(94\)90336-0](https://doi.org/10.1016/0092-8674(94)90336-0)
- Glennon, E. E., Restif, O., Sbarbaro, S. R., Garnier, R., Cunningham, A. A., Suu-Ire, R. D., ... Peel, A. J. (2018). Domesticated animals as hosts of henipaviruses and filoviruses: A systematic review. *The Veterinary Journal*, 233, 25–34. doi:[10.1016/j.tvjl.2017.12.024](https://doi.org/10.1016/j.tvjl.2017.12.024)
- Grote, A., Hiller, K., Scheer, M., Munch, R., Nortemann, B., Hempel, D. C., & Jahn, D. (2005). JCat: A novel tool to adapt codon usage of a target gene to its potential expression host. *Nucleic Acids Research*, 33(Web Server), W526–531. doi:[10.1093/nar/gki376](https://doi.org/10.1093/nar/gki376)
- Gupta, N., Khatoon, N., Mishra, A., Verma, V. K., & Prajapati, V. K. (2019). Structural vaccinology approach to investigate the virulent and secretory proteins of *Bacillus anthracis* for devising anthrax next-generation vaccine. *Journal of Biomolecular Structure and Dynamics*, 1–11. doi:[10.1080/07391102.2019.1688197](https://doi.org/10.1080/07391102.2019.1688197)
- Hasan, M., Islam, S., Chakraborty, S., Mustafa, A. H., Azim, K. F., Joy, Z. F., ... Hasan, M. N. (2019). Contriving a chimeric polyvalent vaccine to prevent infections caused by herpes simplex virus (type-1 and type-2): An exploratory immunoinformatic approach. *Journal of Biomolecular Structure and Dynamics*, 1–18. doi:[10.1080/07391102.2019.1647286](https://doi.org/10.1080/07391102.2019.1647286)
- Heo, L., Park, H., & Seok, C. (2013). GalaxyRefine: Protein structure refinement driven by side-chain repacking. *Nucleic Acids Research*, 41(W1), W384–388. doi:[10.1093/nar/gkt458](https://doi.org/10.1093/nar/gkt458)
- Kamthania, M., & Sharma, D. K. (2015). Screening and structure-based modeling of T-cell epitopes of Nipah virus proteome: An immunoinformatic approach for designing peptide-based vaccine. *3 Biotech*, 5(6), 877–882. doi:[10.1007/s13205-015-0303-8](https://doi.org/10.1007/s13205-015-0303-8)
- Khatoon, N., Pandey, R. K., Ojha, R., Aathmanathan, V. S., Krishnan, M., & Prajapati, V. K. (2019). Exploratory algorithm to devise multi-epitope subunit vaccine by investigating *Leishmania donovani* membrane proteins. *Journal of Biomolecular Structure and Dynamics*, 37(9), 2381–2393. doi:[10.1080/07391102.2018.1484815](https://doi.org/10.1080/07391102.2018.1484815)

- Kong, D., Wen, Z., Su, H., Ge, J., Chen, W., Wang, X., ... Bu, Z. (2012). Newcastle disease virus-vectored Nipah encephalitis vaccines induce B and T cell responses in mice and long-lasting neutralizing antibodies in pigs. *Virology*, 432(2), 327–335. doi:[10.1016/j.virol.2012.06.001](https://doi.org/10.1016/j.virol.2012.06.001)
- Kozakov, D., Hall, D. R., Xia, B., Porter, K. A., Padhorny, D., Yueh, C., ... Vajda, S. (2017). The ClusPro web server for protein-protein docking. *Nature Protocols*, 12(2), 255–278. doi:[10.1038/nprot.2016.169](https://doi.org/10.1038/nprot.2016.169)
- Kumar, N., Singh, A., Grover, S., Kumari, A., Kumar Dhar, P., Chandra, R., & Grover, A. (2019). HHV-5 epitope: A potential vaccine candidate with high antigenicity and large coverage. *Journal of Biomolecular Structure and Dynamics*, 37(8), 2098–2109. doi:[10.1080/07391102.2018.1477620](https://doi.org/10.1080/07391102.2018.1477620)
- Larsen, M. V., Lundsgaard, C., Lamberth, K., Buus, S., Lund, O., & Nielsen, M. (2007). Large-scale validation of methods for cytotoxic T-lymphocyte epitope prediction. *BMC Bioinformatics*, 8(1), 424. doi:[10.1186/1471-2105-8-424](https://doi.org/10.1186/1471-2105-8-424)
- Laskowski, R. A., MacArthur, M. W., Moss, D. S., & Thornton, J. M. (1993). PROCHECK: A program to check the stereochemical quality of protein structures. *Journal of Applied Crystallography*, 26(2), 283–291. doi:[10.1107/S0021889892009944](https://doi.org/10.1107/S0021889892009944)
- Lo, M. K., Bird, B. H., Chattopadhyay, A., Drew, C. P., Martin, B. E., Coleman, J. D., ... Spiropoulou, C. F. (2014). Single-dose replication-defective VSV-based Nipah virus vaccines provide protection from lethal challenge in Syrian hamsters. *Antiviral Research*, 101, 26–29. doi:[10.1016/j.antiviral.2013.10.012](https://doi.org/10.1016/j.antiviral.2013.10.012)
- Magnan, C. N., Zeller, M., Kayala, M. A., Vigil, A., Randall, A., Felgner, P. L., & Baldi, P. (2010). High-throughput prediction of protein antigenicity using protein microarray data. *Bioinformatics*, 26(23), 2936–2943. doi:[10.1093/bioinformatics/btq551](https://doi.org/10.1093/bioinformatics/btq551)
- McEachern, J. A., Bingham, J., Crameri, G., Green, D. J., Hancock, T. J., Middleton, D., ... Bossart, K. N. (2008). A recombinant subunit vaccine formulation protects against lethal Nipah virus challenge in cats. *Vaccine*, 26(31), 3842–3852. doi:[10.1016/j.vaccine.2008.05.016](https://doi.org/10.1016/j.vaccine.2008.05.016)
- McGuffin, L. J., Bryson, K., & Jones, D. T. (2000). The PSIPRED protein structure prediction server. *Bioinformatics*, 16(4), 404–405. doi:[10.1093/bioinformatics/16.4.404](https://doi.org/10.1093/bioinformatics/16.4.404)
- Mehand, M. S., Al-Shorbaji, F., Millett, P., & Murgue, B. (2018). The WHO R&D Blueprint: 2018 review of emerging infectious diseases requiring urgent research and development efforts. *Antiviral Research*, 159, 63–67. doi:[10.1016/j.antiviral.2018.09.009](https://doi.org/10.1016/j.antiviral.2018.09.009)
- Mire, C. E., Versteeg, K. M., Cross, R. W., Agans, K. N., Fenton, K. A., Whitt, M. A., & Geisbert, T. W. (2013). Single injection recombinant vesicular stomatitis virus vaccines protect ferrets against lethal Nipah virus disease. *Virology Journal*, 10(1), 353. doi:[10.1186/1743-422X-10-353](https://doi.org/10.1186/1743-422X-10-353)
- Mohd Nor, M. N., Gan, C. H., & Ong, B. L. (2000). Nipah virus infection of pigs in peninsular Malaysia. *Revue Scientifique et Technique de L'ole*, 19(1), 160–165. doi:[10.20506/rst.19.1.1202](https://doi.org/10.20506/rst.19.1.1202)
- Nain, Z., Abdulla, F., Rahman, M. M., Karim, M. M., Khan, M. S. A., Sayed, S. B., ... Adhikari, U. K. (2019). Proteome-wide screening for designing a multi-epitope vaccine against emerging pathogen Elizabethkingia anophelis using immunoinformatic approaches. *Journal of Biomolecular Structure and Dynamics*, 1–18. doi:[10.1080/07391102.2019.1692072](https://doi.org/10.1080/07391102.2019.1692072)
- Ong, K. C., & Wong, K. T. (2015). Henipavirus Encephalitis: Recent Developments and Advances. *Brain Pathology*, 25(5), 605–613. doi:[10.1111/bpa.12278](https://doi.org/10.1111/bpa.12278)
- Oppenheim, J. J., Biragyn, A., Kwak, L. W., & Yang, D. (2003). Roles of antimicrobial peptides such as defensins in innate and adaptive immunity. *Ann Rheum Dis*, 62(Suppl 2), ii17–21. doi:[10.1136/ard.62.suppl_2.ii17](https://doi.org/10.1136/ard.62.suppl_2.ii17)
- Parveg, M. M., Rahman, M., Nibir, Y. M., & Hossain, M. S. (2016). Two highly similar LAEDDTNAQKT and LTDKIGTEI epitopes in G glycoprotein may be useful for effective epitope based vaccine design against pathogenic Henipavirus. *Computational Biology and Chemistry*, 61, 270–280. doi:[10.1016/j.combiolchem.2016.03.001](https://doi.org/10.1016/j.combiolchem.2016.03.001)
- Pasala, C., Chilamakuri, C. S. R., Katari, S. K., Nalamolu, R. M., Bitla, A. R., & Amineni, U. (2019). Epitope-driven common subunit vaccine design against *H. pylori* strains. *Journal of Biomolecular Structure and Dynamics*, 37(14), 3740–3750. doi:[10.1080/07391102.2018.1526714](https://doi.org/10.1080/07391102.2018.1526714)
- People, N. I., Group, H. S., Bhargava, B., Arunkumar, G., Mourya, D. T., Sadanandan, R., ... Singh, S. K. (2018). Outbreak Investigation of Nipah Virus Disease in Kerala, India, 2018. doi:[10.1093/infdis/jiy612](https://doi.org/10.1093/infdis/jiy612)
- Phillips, J. C., Braun, R., Wang, W., Gumbart, J., Tajkhorshid, E., Villa, E., ... Schulten, K. (2005). Scalable molecular dynamics with NAMD. *Journal of computational Chemistry*, 26(16), 1781–1802. doi:[10.1002/jcc.20289](https://doi.org/10.1002/jcc.20289)
- Prescott, J., DeBuysscher, B. L., Feldmann, F., Gardner, D. J., Haddock, E., Martellaro, C., ... Feldmann, H. (2015). Single-dose live-attenuated vesicular stomatitis virus-based vaccine protects African green monkeys from Nipah virus disease. *Vaccine*, 33(24), 2823–2829. doi:[10.1016/j.vaccine.2015.03.089](https://doi.org/10.1016/j.vaccine.2015.03.089)
- Ravichandran, L., Venkatesan, A., & Febin Prabhu Dass, J. (2019). Epitope-based immunoinformatics approach on RNA-dependent RNA polymerase (RdRp) protein complex of Nipah virus (NiV). *Journal of Cellular Biochemistry*, 120(5), 7082–7095. doi:[10.1002/jcb.27979](https://doi.org/10.1002/jcb.27979)
- Sabetian, S., Nezafat, N., Dorosti, H., Zarei, M., & Ghasemi, Y. (2019). Exploring dengue proteome to design an effective epitope-based vaccine against dengue virus. *Journal of Biomolecular Structure and Dynamics*, 37(10), 2546–2563. doi:[10.1080/07391102.2018.1491890](https://doi.org/10.1080/07391102.2018.1491890)
- Saha, C. K., Mahbub Hasan, M., Saddam Hossain, M., Asraful Jahan, M., & Azad, A. K. (2017). In silico identification and characterization of common epitope-based peptide vaccine for Nipah and Hendra viruses. *Asian Pacific Journal of Tropical Medicine*, 10(6), 529–538. doi:[10.1016/j.apjtm.2017.06.016](https://doi.org/10.1016/j.apjtm.2017.06.016)
- Saha, S., & Raghava, G. P. S. (2006). AlgPred: Prediction of allergenic proteins and mapping of IgE epitopes. *Nucleic Acids Research*, 34(Web Server), W202–W209. doi:[10.1093/nar/gkl343](https://doi.org/10.1093/nar/gkl343)
- Sakib, M. S., Islam, M. R., Hasan, A. K. M. M., & Nabi, A. H. M. N. (2014). Prediction of Epitope-Based Peptides for the Utility of Vaccine Development from Fusion and Glycoprotein of Nipah Virus Using In Silico Approach. *Advances in Bioinformatics*, 2014, 1–17. doi:[10.1155/2014/402492](https://doi.org/10.1155/2014/402492)
- Satterfield, B. A., Cross, R. W., Fenton, K. A., Agans, K. N., Basler, C. F., Geisbert, T. W., & Mire, C. E. (2015). The immunomodulating V and W proteins of Nipah virus determine disease course. *Nature Communications*, 6(1), 7483–7483. doi:[10.1038/ncomms8483](https://doi.org/10.1038/ncomms8483)
- Satterfield, B. A., Dawes, B. E., & Milligan, G. N. (2016). Status of vaccine research and development of vaccines for Nipah virus. *Vaccine*, 34(26), 2971–2975. doi:[10.1016/j.vaccine.2015.12.075](https://doi.org/10.1016/j.vaccine.2015.12.075)
- Satterfield, B. A., Geisbert, T. W., & Mire, C. E. (2016). Inhibition of the host antiviral response by Nipah virus: Current understanding and future perspectives. *Future Virology*, 11(5), 331–344. doi:[10.2217/fvl-2016-0027](https://doi.org/10.2217/fvl-2016-0027)
- Shaw, M. L., Cardenas, W. B., Zamarripa, D., Palese, P., & Basler, C. F. (2005). Nuclear Localization of the Nipah Virus W Protein Allows for Inhibition of both Virus- and Toll-Like Receptor 3-Triggered Signaling Pathways. *Journal of Virology*, 79(10), 6078–6088. doi:[10.1128/JVI.79.10.6078-6088.2005](https://doi.org/10.1128/JVI.79.10.6078-6088.2005)
- Shaw, M. L., García-Sastre, A., Palese, P., & Basler, C. F. (2004). Nipah virus V and W proteins have a common STAT1-binding domain yet inhibit STAT1 activation from the cytoplasmic and nuclear compartments, respectively. *Journal of Virology*, 78(11), 5633–5641. doi:[10.1128/JVI.78.11.5633-5641.2004](https://doi.org/10.1128/JVI.78.11.5633-5641.2004)
- Srivastava, S., Kamthan, M., Kumar Pandey, R., Kumar Saxena, A., Saxena, V., Kumar Singh, S., ... Sharma, N. (2019). Design of novel multi-epitope vaccines against severe acute respiratory syndrome validated through multistage molecular interaction and dynamics. *Journal of Biomolecular Structure and Dynamics*, 37(16), 4345–4360. doi:[10.1080/07391102.2018.1548977](https://doi.org/10.1080/07391102.2018.1548977)
- Tosta, S. F. D. O., Passos, M. S., Kato, R., Salgado, Á., Xavier, J., Jaiswal, A. K., ... Alcantara, L. C. J. (2019). Multi-epitope based vaccine against yellow fever virus applying immunoinformatics approaches. *Journal of Biomolecular Structure and Dynamics*, 1–17. doi:[10.1080/07391102.2019.1707120](https://doi.org/10.1080/07391102.2019.1707120)
- Ul-Rahman, A., & Shabbir, M. A. B. (2019). In silico analysis for development of epitopes-based peptide vaccine against Alkhurma hemorrhagic fever virus. *Journal of Biomolecular Structure and Dynamics*, 1–13. doi:[10.1080/07391102.2019.1651673](https://doi.org/10.1080/07391102.2019.1651673)

- Wang, P., Sidney, J., Dow, C., Mothe, B., Sette, A., & Peters, B. (2008). A systematic assessment of MHC class II peptide binding predictions and evaluation of a consensus approach. *PLoS Computational Biology*, 4(4), e1000048. doi:[10.1371/journal.pcbi.1000048](https://doi.org/10.1371/journal.pcbi.1000048)
- Weatherman, S., Feldmann, H., & de Wit, E. (2018). Transmission of henipaviruses. *Current Opinion in Virology*, 28, 7–11. doi:[10.1016/j.coviro.2017.09.004](https://doi.org/10.1016/j.coviro.2017.09.004)
- Weingartl, H. M., Berhane, Y., Caswell, J. L., Loosmore, S., Audonnet, J.-C., Roth, J. A., & Czub, M. (2006). Recombinant Nipah Virus Vaccines Protect Pigs against Challenge. *Journal of Virology*, 80(16), 7929–7938. doi:[10.1128/JVI.00263-06](https://doi.org/10.1128/JVI.00263-06)
- Wilkins, M. R., Gasteiger, E., Bairoch, A., Sanchez, J. C., Williams, K. L., Appel, R. D., & Hochstrasser, D. F. (1999). Protein identification and analysis tools in the ExPASy server. *Methods in Molecular Biology* (Clifton, N.J.), 112, 531–552. doi:[10.1385/1-59259-584-7:531](https://doi.org/10.1385/1-59259-584-7:531) [10027275]
- Wu, F., Bhansali, S. G., Law, W. C., Bergey, E. J., Prasad, P. N., & Morris, M. E. (2012). Fluorescence imaging of the lymph node uptake of proteins in mice after subcutaneous injection: Molecular weight dependence. *Pharmaceutical Research*, 29(7), 1843–1853. doi:[10.1007/s11095-012-0708-6](https://doi.org/10.1007/s11095-012-0708-6)
- Yang, J., Yan, R., Roy, A., Xu, D., Poisson, J., & Zhang, Y. (2015). The iTASSER Suite: Protein structure and function prediction. *Nature Methods*, 12(1), 7–8. doi:[10.1038/nmeth.3213](https://doi.org/10.1038/nmeth.3213)
- Yin, S., Ding, F., & Dokholyan, N. V. (2007). Eris: An automated estimator of protein stability. *Nature Methods*, 4(6), 466–467. doi:[10.1038/nmeth0607-466](https://doi.org/10.1038/nmeth0607-466)